공학박사학위논문

Synthesis and Characterization of Allyl Polysulfone Derivatives for Membrane Application and Polystyrene Sulfonate Derivatives for Draw Solute Application

수처리 분리막 응용을 위한 알릴 폴리술폰 유도체 및 유도용질로의 응용을 위한 폴리스티렌 술폰산 유도체의 합성과 분석

2017년 2월

서울대학교 대학원

화학생물공학부

김 진 주

수처리 분리막 응용을 위한 알릴 폴리술폰 유도체 및 유도 용질로의 응용을 위한 폴리스티렌 술폰산 유도체의 합성과 분석

Synthesis and Characterization of Allyl Polysulfone Derivatives for Membrane Application and Polystyrene Sulfonate Derivatives for Draw Solute Application

지도교수 이 종 찬 박사

이 논문을 공학박사학위 논문으로 제출함.

2017 년 2 월

서울대학교 대학원

화학생물공학부

김 진 주

김진주의 박사학위논문을 인준함.

2017 년 2 월

위 원 장 장 정 식 (인)

부위원장 이 종찬 (인)

위 원 조 재영 (인)

위 원 안 철희 (인)

위 원 이 중희 (인)

Synthesis and Characterization of Allyl Polysulfone Derivatives for Membrane Application and Polystyrene Sulfonate Derivatives for Draw Solute Application

by

Jin-joo Kim

Adviser: Professor Jong-Chan Lee, Ph. D.

Submitted in Partial Fulfillment
of the Requirements for the Degree of
DOCTOR OF PHILOSOPHY

February 2017

School of Chemical and Biological Engineering
College of Engineering
Graduate School
Seoul National University

Abstract

This study presents synthesis and characterization of novel polymeric materials and their application to water treatment. Firstly, A series of ultrafiltration (UF) membranes based on polysulfone and mussel-inspired poly(dopamine methacrylamide) (PDMA) were prepared by a versatile *in situ* process composed of *grafting-through* polymerization and consecutive non-solvent induced phase separation. Nisin, a low molecular weight antimicrobial peptide, was subsequently immobilized on the surface of the UF membrane through the reaction between its N-terminal NH_2 group and the catechol group in PDMA for microbial mitigation. The resulting nisin containing UF membranes showed outstanding fouling resistance and flux recovery ability due to the hydrophilic characteristics of PDMA moiety in the membrane. Furthermore, it is worth noting that the resulting membranes exhibit the antimicrobial activity against the *Staphylococcus aureus* (ATCC 6538) due to the nisin moiety.

Second, thin film composite (TFC) polyamide membrane with tailored support structure was prepared for forward osmosis (FO) application. The porous polysulfone-based substrate was fabricated using the *grafting-through* polymerization of allyl polysulfone and dimethylaminoethyl methacrylate (DMAEMA), followed by non-solvent induced phase separation. 1,3,5-tricarbonyl

trichloride and *m*-phenylene diamine were employed as the monomers for the interfacial polymerization to form a thin polyamide selective layer. poly(dimethylaminoethyl methacrylate) (PDMAEMA) moieties in the substrate was then convert into zwitterionic sulfobetaine moieties to impart fouling resistance. When the TFC membrane prepared in this study was tested in the FO system, a remarkably large water permeation flux value (~63.2 LMH) was observed with a small ratio of reverse solute flux to water permeation flux (J_s/J_v) of < 0.02 g/L in the active layer against draw solution (AL-DS) mode using 2 M NaCl solution as a draw solution and DI water as a feed solution. Especially, the zwitterionic substrate in the TFC membrane exhibited fouling resistance against synthetic wastewater feed stream.

Third, a series of oligomeric poly(tetrabutylphosphonium styrenesulfonate)s (PSSP#, where # is the number of monomer units in the oligomer) were prepared from tetrabutylphosphonium styrenesulfonate (SSP) as a monomer for application as a draw solute in a FO system. Although the water permeation flux values in the FO system using the oligomeric PSSP as a draw solute were slightly smaller than those using the monomeric SSP, the reverse solute flux values using the PSSPs were found to be much smaller than those using the SSP, indicating that the oligomers are more efficient draw solute materials in the FO system than the low molecular weight monomer. For example, when 20 wt% of the PSSP5 aqueous

solution is used as the draw solution, the water permeation flux and reverse solute flux values are 14.50 LMH and 0.14 gMH, respectively, and when 20 wt% of the SSP aqueous solution is used, they are 16.28 LMH and 0.53 gMH, respectively. Since PSSPs have a lower critical solution temperature (LCST), the PSSP in water could be simply separated by heating to above the LCST without any other separation process. Moreover, it was found that the PSSPs have excellent bactericidal property above 99.9 % against *Escherichia coli* (ATCC 8739).

Keyword: Water treatment, membrane, draw solute, forward osmosis, ultrafiltration, antifouling

Student Number: 2010-23327

TABLE OF CONTENT

Chapter 2

Antifouling and Antimicrobial Membranes for Ultrafiltration (UF) Application

Chapter 3

Thin Film Composite (TFC) Membranes for Forward Osmosis (FO) Application

Chapter 4

Oligomeric Draw Solutes for FO Application

List of Figures

List of Tables

Chapter 1

Introduction

1.1. Membranes for ultrafiltration (UF) process

Membrane filtration processes have attracted much attention, driven by increasing needs in water treatment, food, chemical, and biochemical industries.[1-3] Ultrafiltration (UF) system is one of the most widely applied filtration process with separating molecules in the pore size range of 5-100 nm. The decrease in water flux caused by membrane fouling has been recognized as a major obstacle in the UF process, because it has detrimental effects on the efficiency and economics of the whole membrane filtration process.[4-5] The membrane fouling originates from the interactions between the membrane surface and foulants such as proteins or microorganisms in the feed stream.[6-7] Furthermore, the growth and colonization of bacteria on the membrane surface degenerate the comprehensive performance of the membrane during storage as well as operation. Although numerous fouling control strategies including turbulent hydrodynamic conditions, biocide pretreatment, and cleaning of the membranes have been demonstrated, these incur extra operational cost.[8-13] Therefore, lots of researches have been focused on the preparation of antifouling and/or antimicrobial membranes to maintain the membrane performance.[14-16]

It has been generally accepted that hydrophilic membranes are resistant to the adhesion of protein or bacteria.[17] Poly(ethylene glycol) (PEG) is one of the

intensively studied as a antifouling polymer due to the its good fouling-resistant properties.[18,19] Poly(N-vinyl pyrrolidone),[20,21] polyglycerol,[22], and polydopamine,[23] have been also studied because of their repulsive interaction with foulants. Recently, mussel-inspired polydopamine (PDA) has attracted much attention because PDA forms hydrogen bonds with water molecules and inhibits the deposition of foulants on the membrane surface and/or inner pores.[23,24]

In order to impart hydrophilicity to the hydrophobic surface of conventional membranes, significant effort has been devoted to develop suitable techniques for the fabrication of antifouling and/or antimicrobial membranes. Recent advances were focused on enhancing the membrane synthesis protocols, modifying the surface properties by grafting functional polymer onto the surface, and on developing nanocomposite membranes by incorporating of nanofillers.[25] Recently, a facial and economical method has recently been developed and widely used to prepare the functional membranes by *in situ* process, which conducts phase separation right after the polymerization without further purification.[26-29]

1.2. Membranes and draw solutes for forward osmosis (FO) process

Global water crisis is the foremost global risk of social, environmental, and economical development of many countries in the next decades. Over the past decade, demand for fresh water has drastically increased with rapid growth in the population, advancement in industrialization, global climate change, and growing scarcity of fresh water.[30] Membrane separation technologies have secured an important role in available water purification as a promising technology for removing multiple sized solutes and organic pollutants from seawater or brackish water. Forward osmosis (FO) is an emerging membrane process which water is diffused from the feed solution (low osmotic potential) to the draw solution (high osmotic potential) by the osmotic pressure gradient between two solutions. Since no external hydraulic pressure is required, FO can be a low energy water separation process if the draw solute can be economically regenerated.[31-32]

There are two major obstacles hindering further development of FO process.[31] First, the lack of a suitable membrane designed specifically for FO process prohibit the wide range of application. Since previous membranes have been designed to exhibit high selectivity in order to apply these membranes as pressure-

driven membrane process. Therefore, most of commercial membranes include thick and hydrophobic porous substrate to withstand extremely high external pressure during the filtration process.[32] However, in osmotic-driven membrane process, application of the above-mentioned membranes demonstrates severe decline of water permeation flux caused from concentration polarization, especially occurred in the porous structure of the substrate. Much attention has been focused on the alleviation of concentration polarization by developing thin and hydrophilic substrate, which is easily wetted in water and accelerates water transport.[33,34]

Second and the most problematic impediment is the lack of appropriate draw solution that generates high osmotic pressure in both operational and economic point of view. The main problems regarding the selection of draw solutes are the significant draw solute leakage during the FO process and/or large energy consumption during draw solute regeneration. Therefore, three primary criteria need to be considered in the selection of draw solutes: (1) high osmotic pressure which may induce fast diffusion of water molecules, (2) minimal reverse solute diffusion from the draw solution to the feed solution which can decrease the replenishing cost, (3) facile regeneration of the diluted draw solution after the membrane module in order to reduce the energy consumption and overall operation cost.[35-37] Good solubility in water, zero toxicity, antimicrobial

property, and low viscosity of the draw solutes are also required in order to exhibit high efficiency in the FO process. Numerous approaches have been investigate to regenerate the draw solute with various strategies such as heat,[38] magnetic field,[35,39] Hot ultrafiltration,[40] membrane distillation.[41]

1.3. Motivation

It is very important issue to develop appropriate synthetic materials for membrane and draw solute application in order to deal with the growing scarcity of surface and ground water resources.[30] Although numerous of candidates have been reported as promising materials with demonstrating prominent performance in ultrafiltration (UF) and forward osmosis (FO) processes, there are many problems to replace conventional systems.[42-44] Therefore, we attempted to prepare novel polymeric mateirals for UF and FO application in this study.

Although the development of antifouling and antimicrobial membranes has been studied extensively,[45] there has been few reports concerning the development of long-lasting antimicrobial membrane surface. Therefore, antifouling and antimicrobial UF membrane was prepared by *in situ* process composed of *grafting-through* polymerization, phase inversion, and consecutive immersion process.[8,11,13] Nisin, a low molecular weight antimicrobial peptide (3,500 g/mol), was covalently bonded onto the membrane surface through the Schiff base formation or Michael addition reaction without degradation of the antimicrobial properties. From systematic investigations on the membrane properties, we found that the resulting membranes exhibited higher fouling

resistance and antimicrobial properties compared to pristine polysulfone membrane.

Porous substrate was also prepared by *in situ* process composed of *grafting-through* polymerization and consecutive phase inversion using allyl polysulfone. After fabricating polyamide selective layer on top of the porous substrate, multilayered thin film composite membrane was prepared exploiting the highly desirable advantages based on the substrate hydrophilicity, which significantly alleviate internal concentration polarization. The substrate was further modified in order to provide zwitterionic moieties after the preparation of the thin film composite membrane, causing the additional enhancement of FO performances and fouling resistance.

Since the practical application of the FO system has been limited due to the absence of adequate draw solutes and their regeneration, early efforts have been investigated on the exploration of draw soutes. We tried to suggest novel thermos-responsive oligoelectrolytes as draw solute for FO application. Their oligomeric molecular weight efficiently inhibit the reverse diffusion of draw solute during the FO process, with exhibiting noticeably high osmotic potential, resulting large water permeation flux and small reverse solute flux. Furthermore, the oligoelectrolytes showed thermo-responsive behavior due to the changes of the interactive forces between water with oligoelectrolytes.[46] Especially, 99.5% of

precipitated oligoelectrtolytes can be recovered by simple pouring process.

1.4. References

[1] Goosen MFA, Sablani SS, Al-Hinai H, Al-Obeidani S, Al-Belushi R, Jakson D. Sep Sci Technol 39 (2004) 2261-2297.

[2] Freeman BD, Pinnau FI. in Advanced Materials for Membrane Separations, American Chemical Society (2004).

[3] Shannon MA, Bohn PW, Elimelech M, Georgiadis JG, Mañas BJ, Mayes AM. Nature, 452 (2008) 301-310.

[4] Hilal N, Ogunbiyi OO, Miles NJ, Nigmatullin R. Sep Sci Technol 40 (2005) 1957-2005.

[5] Mansouri J, Harrisson S, Chen V. J Mater Chem 20 (2010) 4567-4586.

[6] Lim AL, Bai R. J Membr Sci 216 (2003) 279-290.

[7] Guo W, Ngo HH, Li J. Bioresource Technol 122 (2012) 27-34.

[8] Kochkodan V. Hilal N. Desalination, 356 (2015) 187-207.

[9] Lotfiyan H, Zokaee Ashtiani F, Fouladitajar A, Armand SB. J Membr Sci 472 (2014) 1-9.

[10] Wu T, Zhou B, Zhu T, Shi J, Xu Z, Hu C, Wang J. RSC Adv 5 (2015) 7880-7889.

[11] Zhao Q, Hou J, Shen J, Liu J, Zhang Y. J Mater Chem A 3 (2015) 18696-

18705.

[12] Loganathan K, Chelme-Ayala P, Gamal El-Din M. Desalination, 360 (2015) 52-60.

[13] Dumée LF, He L, King PC, Moing ML, Güller I, Duke M, Hodgson PD, Gray S, Poole AJ, Kong L. J Membr Sci 475 (2015) 552-561.

[14] Kim D-G, Kang H, Han S, Kim HJ, Lee J-C. RSC Adv 3 (2013) 18071-18081.

[15] Kim D-G, Kang H, Han S, Lee J-C. ACS Appl Mater Interfaces 4 (2012) 5898-5906.

[16] Kim D-G, Kang H, Han S, Lee J-C. J Mater Chem 22 (2012) 8654-8661.

[17] Parra C, Montero-Silva F, Henríquez R, Flores M, Garín C, Ramírez C, Moreno M, Correa J, Seeger J, Häberle P. ACS Appl Mater and Interfaces 7 (2015) 6430-6437.

[18] Hucknall A, Rangarajan S, Chilkoti A. Adv Mater 21 (2009) 2441-2446.

[19] Prime KL, Whitesides GM. Science 252 (1991) 1164-1167.

[20] Qin JJ, Cao YM, Li YQ, Li Y, Oo MH, Lee H. Sep Purif Technol 36 (2004) 149-155.

[21] Huang X, Wang W, Liu Y, Wang H, Zhang Z, Fan W, Li L. Chem Eng J 273 (2015) 421-429.

[22] Li X, Cai T, Chung T-S. Environ Sci Technol 48 (2014) 9898-9907.

[23] Choi Y-S, Kang H, Kim D-G, Cha S-H, Lee J-C. ACS Appl Mater Interfaces 6 (2014) 21297-21307.

[24] McCloskey BD, Park HB, Ju H, Rowe BW, Miller DJ, Chun BJ, Kin K, Freeman BD. Polymer 51 (2010) 3472-3485.

[25] Liu F, Hashim NA, Liu Y, Abed MRM, Li K. J Membr Sci 375 (2011) 1-27.

[26] Zhang P-Y, Xu Z-L, Yang H, Wei Y-M, Wu W-Z. Chem Eng Sci 97 (2013) 296-308.

[27] Qin H, Sun C, He C, Wang D, Cheng C, Nie S, Sun S, Zhao C. J Membr Sci 468 (2014) 172-183.

[28] Xiang T, Luo C-D, Wang R, Han Z-Y, Sun S-D, Zhao C-S. J Membr Sci 476 (2015) 234-242.

[29] Cheng C, He A, Nie C, Xia Y, He C, Ma L, Zhao C. J Mater Chem B 3 (2015) 4170-4180.

[30] M. Hightower, S.A. Pierce, The energy challenge, Nature, 452 (2008) 285-286.

[31] Nagy E. J Membr Sci 460 (2014) 71-81.

[32] McCutcheon JR, Elimelech M. J Membr Sci 318 (2008) 458-466.

[33] Chekli L, Phuntsho S, Shon HK, Vigneswaran S, Kandasamy J, Chanan A. Desalin Water Treat 43 (2012) 167-184.

[34] Li D, Wang H. J Mater Chem A 1 (2013) 14049-14060.

[35] Ling MM, Wang KY, Chung T-S. Ind Eng Chem Res 49 (2010) 5869-5876.

[36] Phuntsho S, Shon HK, Hong S, Lee S, Vigneswaran S. J Membr Sci 375 (2011) 172-181.

[37] Achilli A, Cath TY, Childress AE. J Membr Sci 364 (2010) 233-241.

[38] McCutcheon JR, McGinnis RL, Elimelech M. Desalination, 174 (2005) 1-11.

[39] Ge Q, Su J, Chung T-S, Amy G. Ind Eng Chem Res 50 (2011) 382-388.

[40] Kim J-j, Chung J-S, Kang H, Yu YA, Choi WJ, Kim HJ, Lee J-C. Macromol Res 22 (2014) 963-970.

[41] Martinetti CR, Childress AE, Cath TY. J Membr Sci 331 (2009) 31-39.

[42] Gao G, Yu K, Kindrachuk J, Brook DE, Hancock REW, Kizhakkedathu JN. Biomacromolecules 12 (2011) 3715-3727.

[43] Chung T-S, Zhang S, Wang KY, Su J, Ling MM. Desalination 287 (2012) 78-81.

[44] Howe KJ, Clark MM. Environ Sci Technol 36 (2002) 3571-3576.

[45] Jiang J, Zhu L, Zhu L, Zhang H, Zhu B, Xu Y. ACS Appl Mater Interfaces 5 (2013) 12895-12904.

[46] Kohno Y, Ohno H. Phys Chem Chem Phys 14 (2012) 5063-5070.

Chapter 2

Antifouling and Antimicrobial Membranes for Ultrafiltration (UF) Application

2.1. Introduction

Polymer membranes have been widely used in a number of important separation technologies including the removal of macromolecules, organic pollutants, bacteria, viruses, salts, and gas molecules from various kinds of feed streams.[1-4] However, significant decline of water flux has been observed in the separation systems based on the polymer membranes because organic pollutants and microorganisms in the feed stream can easily deposit onto the membrane surface and/or in its pore walls composed of organic moieties.[5,6] Furthermore, the growth and colonization of bacteria on the membrane degenerate the comprehensive performances of the membrane during storage as well as operation. Therefore, a number of approaches to prepare antifouling and/or antimicrobial membranes have been studied to maintain the membrane performance.[7-9]

It was found that the increase of membrane hydrophilicity could alleviate the fouling due to their attenuated interaction between the membrane surface and foulants.[10-12] Therefore, the introduction of hydrophilic polymers including poly(ethylene glycol) (PEG),[7-9,13] poly(N-vinyl pyrrolidone) (PVP),[14,15], polyglycerol (PG)[16], and polydopamine (PDA)[17] have attracted a great deal of attention due to their repulsive interaction with foulants. Especially, the catechol groups in PDA forming hydrogen bonds with water molecules were

found to inhibit the deposition of foulants on the membrane surface and/or inner pores.[17,18] Furthermore, the catechol groups can be oxidized into the reactive quinones under basic conditions, then they can be reacted with the amine groups of antimicrobial peptides.[19,20] Although antimicrobial peptides have been known to prevent the growth of bacteria effectively due to its broad activity, rapid action, and low side effect,[21-23] membranes immobilized with the peptides have not been widely used due to the lack of the long-term stability caused by the release of the peptides. Obviously the release problem could be overcome by immobilizing the antimicrobial peptides through the covalent bonding on the membrane surface.[20]

In this study we prepared antifouling and antimicrobial polysulfone-based ultrafiltration (UF) membrane by introducing the PDA moiety for the antifouling property through the in situ process[33-37] and by immobilizing nisin as an antimicrobial peptide through post treatment.[20] The surface properties, fouling resistance, and antimicrobial properties of the membranes containing PDA and nisin moieties were investigated and compared to those of bare polysulfone (PSf) membrane.

2.2. Experimental

Materials

2,2'-Diallylbisphenol A (DBPA, 85.0%) was purchased from Sigma-Aldrich Co., LLC. and purified by the procedure reported before.[44] Bovine serum albumin (BSA) was also purchased from Sigma-Aldrich Co., LLC. and used as received. 4,4'-Difluorodiphenyl sulfone (DFDPS, 99.0%) was obtained from Tokyo Chemical Industry Co., Ltd. and recrystallized from toluene prior to use. Dopamine methacrylamide (DMA) was synthesized by certain procedure as reported previously.[17] 2,2'-Azobis(isobutyronitrile) (AIBN) was purchased from Junsei Chemical Co., Ltd. and purified by recrystallization from ethanol. Methacrylate anhydride (94.0%) was purchased from Alfa Aesar Co., Inc. and used without further purification. *N*-Methyl-2-pyrrolidone (NMP, 99.0%) and toluene (99.0%) were purchased from Junsei Chemical Co., Ltd. and dried over a molecular sieve (4Å). Sodium hydroxide (NaOH, 97.0%) and n-hexane were obtained from Daejung Chemicals & Metals Co., Ltd. and used as received. Tetrahydrofuran (THF, 99.0%) was also purchased from Daejung Chemicals & Metals Co. Ltd. and distilled by refluxing over sodium/benzophenone under a nitrogen adkfemfltmosphere. Polysulfone (PSf, Udel® P-1700) was kindly

supplied by Solvay Advanced Polymers. Nisin (2.5%) was purchased from Wuhan Yuancheng Technology Development Co. Ltd. and used as received. Deionized (DI) water was obtained from water purification system (Synergy, Millipore, USA), having a resistivity of 18.3 MΩ cm. *Staphylococcus aureus* (*S. Aureus*, ATCC 6538) were obtained from American Type Culture Collection (ATCC). Bacto agar and Difco tryptic soy broth were obtained from Becton, Dickinson and Co. (BD). All other reagents and solvents were used as received.

Synthesis of allyl polysulfone (APSf) macromonomer

Allyl polysulfone (APSf) was synthesized by the condensation polymerization of DBPA with DFDPS, as shown in Figure 2.1.[23,45] A 250 mL three neck round bottom flask equipped with an overhead mechanical stirrer, a Dean-Stark trap, and nitrogen inlet and outlet was charged with DBPA (3.08 g, 10 mmol), DFDPS (2.54 g, 10 mmol), K2CO3 (1.52 g, 11 mmol), and hydroquinone (0.011 g, 0.1 mmol) in 6 mL of NMP. Then 3mL of toluene (NMP/toluene = 2/1 v/v) was added as an azeotropic agent. The reaction mixture was refluxed at 140 ^{o}C for 6 h to dehydrate the system. After the toluene was removed at 150 ^{o}C for 4 h, this temperature was maintained for the polymerization. During the polymerization, the reaction mixture turned to a viscous brown solution. The viscous solution was obtained

after 16 h of the reaction, and then it was cooled to room temperature and diluted with 10 mL of NMP. The polymer was obtained by precipitation in isopropyl alcohol, followed by washing with DI water and isopropyl alcohol alternately for several times to completely remove the residual salts and solvent. The number average molecular weight (M_n) and polydispersity index (PDI) were 5,300 g/mol and 1.390, respectively.

^{1}H NMR (400 MHz, $CDCl_3$, TMS ref): δ = 1.66 (6 H, m, -CH_3 of DBPA), 3.23 (2 H, d, -*CH_2*-CH=CH_2 of allyl groups), 4.95 (4 H, m, -CH_2-CH=*CH_2* of allyl groups), 5.70-6.19 (2 H, m, -CH_2-*CH*=CH_2 of allyl groups), 6.93 (4 H, m, ArH ortho to -O-), 7.93 (4 H, d, ArH ortho to -SO_2-), 7.42 (2 H, s, ArH ortho to allyl groups), 6.38-7.94 (m, other ArH).

Preparation of allyl polysulfone-*graft*-poly(dopamine methacrylamide) membrane (AP-DM# membrane)

A series of allyl polysulfone-graft-poly(dopamine methacrylamide) membranes (AP-DM# membranes, where # is the weight ratio of DMA to APSf) membranes were prepared by *in situ* process composed of *grafting-through* polymerization followed by non-solvent induced phase separation (NIPS) method.[35,36] For the preparation of AP-DM1 membrane, APSf (1.00 g), AIBN (0.10 g), PSf (1.00 g),

and DMA (1.00 g) were dissolved in 10.3 mL of NMP in a 100 mL dried Schlenk flask containing a magnetic stir bar. PSf is the commercial polysulfone and it was intentionally used to increase the stability of the membrane. The flask was sealed with a septum and deoxygenate with nitrogen for 1h. The flask was then placed in an oil bath maintained at 80 ^{o}C and stirred with a magnetic stir bar for 6 h for the polymerization of vinylic monomer moieties in APSf and DMA, resulting in a clear brown solution. After the polymerization, the resulting solution was left in sonication at degassing mode for 2 h to remove air bubbles trapped within the solution, followed by casting on a non-woven polyethylene terephthalate (PET) fabric using a doctor blade at a thickness of 200 μm, and then immersed into DI water bath at room temperature. After 24 h, the resulting membrane was rinsed thoroughly for 24 h with 0.25M of NaOH solution to remove the solvent and any remaining poly(dopamine methacrylamide) (PDMA) homopolymer. The resulting membrane was designated as AP-DM1 membrane and the number 1 indicates the weight ratio of DMA to APSf. Other AP-DM# membranes were prepared using the same procedure, except the amount of DMA as listed in Table 2.1.

Preparation of nisin immobilized AP-DM#-N1 and AP-DM#-N5 membranes

An antimicrobial peptide, nisin, was immobilized onto the surface of AP-DM# membranes by the reaction between N-terminal NH2 group of nisin and catechol group of DMA repeat unit. 1.0 g/L and 5.0 g/L of nisin solutions were prepared using 40 and 200 g of nisin powder, respectively, and 1 L of phosphate buffer solution with pH value of 7.4.[20] Since the content of nisin active ingredient is about 2.5%, 40 and 200 g of nisin powder was used to prepared the 1.0 g/L and 5.0 g/L solutions, respectively, followed by removing insoluble component using vacuum filtration in order to prohibit any unintended reaction. In order to immobilize the nisin, the AP-DM# membranes were immersed in the nisin solution for 6 h at room temperature, and then they were rinsed with the phosphate buffer. The rinsed membranes were finally immersed in DI water bath at room temperature at least 24 h, and stored in DI water in the refrigerator. The membranes were named as AP-DM#-N1 and AP-DM#-N5 membranes in accordance with the concentration of nisin active ingredient. The content of nisin in the AP-DM#-N1 and AP-DM#-N5 membranes was estimated by calculating bonding density using Equation(2.1) as follows:

$$\text{Bonding density (\%)} = \frac{W_{memb,t} - W_{memb,t_0}}{A_{memb}} \times 100 \qquad (1)$$

Where $W_{memb,t}$ (μg), A_{memb,t_0} (cm^2), and A_{memb} (cm^2) indicate the weight of membrane at time t, the weight of membrane at initial time t_0, and area of membrane, respectively.

Membrane filtration experiments

Membrane filtration experiments were carried out using a dead-end filtration cell (CF042, Sterlitech Corp., Kent, WA) with an effective membrane area of 5.73 cm^2. All the experiments were carried out under a trans-membrane pressure of 1 bar at room temperature and at an agitating speed of 200 rpm. Pure water permeability (PWP) values of the membrane were obtained from filtering DI water through the membrane for 1 h. For the fouling resistance test, BSA was selected as a model protein and dispersed in phosphate buffer solution (1.0 g/L, pH 7.0) was forced to permeate through the membrane, and the water flux was calculated by measuring the weight of permeated water at a given time. The water flux, Jw ($Lm^{-2}h^{-1}$, designated as LMH), was calculated using Equation (2.2):

$$J_w = \Delta V / (A \times \Delta t) \qquad (2.2)$$

where ΔV (L) is the volume of permeated solution collected between two weight measurements, A (m^2) is the membrane surface area, and Δt (h) is the time between two weight measurements. The flux decline ratio (DR) of the membrane

was calculated as follows:

$$DR\ (\%) = (1 - J_{w,60}/J_{w,0}) \times 100 \quad (2.3)$$

where $J_{w,60}$ (LMH) is the flux recorded after 60 min of dead-end filtration and $J_{w,0}$ (LMH) is the initial flux. The smaller *DR* value indicates the better antifouling property. To investigate the flux recovery ability of the membrane, the membranes were rinsed with DI water at 60 min after initial filtration of the BSA solution. After then, water flux values were measured again with the cleaned membrane and recorded at each time. Flux recovery ratio (*FRR*) was evaluated using Equation (2.4):

$$FRR\ (\%) = (J_{w2}/J_{w,60}) \times 100 \quad (2.4)$$

where J_{w2} (LMH) is the water flux recorded with the cleaned membranes at 60 min after filtration of the initial filtration. The larger *FRR* value indicates the better antifouling property of the membrane. All the filtration experiments for each sample were carried out more than three times to confirm the reproducibility, and the average values were used as the data.

Characterization

The chemical structure of the monomers and polymers was characterized by ^{1}H NMR spectroscopy (ZEOL LNM-LA 300, 30 MHz) using CDCl3 as a solvent. M_n and PDI were analyzed by gel permeation chromatography (GPC) equipped with a Waters 515 HPLC pump and three columns including PLgel 5.0 μm guard, MIXED-C, and MIXED-D from Polymer Laboratories in a series with a refractive index (RI) detector (Viscotek LR125 laser refractometer). The resulting data were calibrated using polystyrene standards from Polymer Laboratories and analyzed using the Omnisec software. HPLC grade THF (J. T. Baker) was used as an eluent at a flow rate of 1.0 mL/min at 35 ^{o}C. Fourier Transform Infrared (FT-IR) spectra were recorded on a Nicolet 6700 spectrophotometer (Thermo Scientific) using attenuated total reflectance (ATR) equipment (FT-IR/ATR). Surface and cross-sectional morphologies of the membranes were investigated by scanning electron microscopy (SEM) using a field emission scanning electron microscope (FESEM, JEOL JSM-6700F) with an accelerating voltage of 10 kV. Before SEM measurement, samples were freeze-dried and coated with platinum using a JEOL JFC-1100E ion sputtering device. The surface atomic composition of the membranes was analyzed by X-ray photoelectron spectroscopy (XPS, Kratos AXIS His) using Mg Kα (1254.0 eV) as a radiation source. XPS spectra were collected over a range of 0-1100 eV, followed by high resolution scan of the C 1s,

O 1s, and N 1s regions. Average pore diameter and pore size distribution the membranes were carried out with a computational analysis (Image-Pro Plus) using SEM images of the membrane surfaces. Contact angle from air captive bubble in water was measured using a contact angle goniometer (Krüss DAS10) Contact angles for the membranes for five times on three independently prepared membranes. The porosity of EC and EP substrates was calculated by measuring the weight of wet and dry membranes. The weight of the wet membrane (m_1, g) was measured, following by freeze dried overnight in order to measure the weight of dry membrane (m_2, g). The overall porosity, ε, could be calculated by the following Equation(2.5):

$$\varepsilon\,(\%) = \frac{(m_1 - m_2)/\rho_w}{(m_1 - m_2)/\rho_w + m_2/\rho_p} \times 100 \qquad (2.5)$$

where ρ_w is the density of water (1 g/cm^3 at 25 ^{o}C) and ρ_p (g/cm^3) is the density of membranes, determined by measuring weight (g) and volume (cm^3) of dry membranes.

Antimicrobial test

The antimicrobial property of the AP-DM#-N1 and AP-DM#-N5 membranes was

tested against *S. aureus* (ATCC 6538) using a shaking flask method. To prepare the bacteria suspension, *S. aureus* was cultured in the corresponding broth solutions for 18 h at 37 ^{o}C. A single colony was lifted off with a platinum loop and placed in 30 mL of nutrient broth, and incubated in a shaking incubator for 18 h at 37 ^{o}C. After washing twice with phosphate buffered saline, the bacterial suspension was diluted to give an initial concentration of a 1×10^6 colony forming unit (CFU) per mL. Bacterial cell concentration was estimated by measuring the absorbance of cell dispersions at 600nm. For evaluating the antimicrobial activity of the AP-DM#-N1 and AP-DM#-N5 membranes, 1×1 cm^2 of the membranes and bare PSf membrane dipped into a Falcon tube containing 5 mL of 1.0 mM phosphate buffered saline culture solution which cell concentration is 1×10^6 CFU/mL The Falcon tubes were then placed in a shaking incubator at 25 ^{o}C for 24 h with a 200 rpm of shaking speed. After vigorous shaking to detach adherent cells from the membrane surfaces, the solution was diluted and then 0.1mL of each diluent was spread onto the corresponding agar plates. Viable microbial colonies were counted after being incubated for 18 h at 37 ^{o}C. Each test was repeated at least three times. The bacterial inhibition rate was obtained as follows:

$$\text{Bacterial inhibition rate (\%)} = \frac{N_0 - N_i}{N_0} \times 100 \qquad (6)$$

where N_0 is the bacterial CFU of the blank sample and N_i is the bacterial CFU of

the tested sample.

2.3. Results and Discussion

Allyl polysulfone (APSf) was synthesized via the condensation polymerization of the dihydroxy monomer (2,2'-diallylbisphenol A (DBPA)) with the dihalo monomer (4,4'-difluorodiphenyl sulfone (DFDPS) where DBPA was intentionally used because the allyl group can go through the radical polymerization to introduce dopamine methacrylamide (DMA) by the *grafting-through* approach. (Figure 2.2). A small amount of hydroquinone as a radical scavenger was added into the reaction mixture in order to prevent unintended isomerization of allyl groups in the DBPA.[13] Figure 2.3 shows ^{1}H NMR spectra and the assignment of the respective peaks of APSf. As expected, all of the corresponding resonance peaks of APSf were clearly found in the spectra (Figure 1). For example, the proton peaks from the allyl groups (δ = 3.23 and 4.95 ppm) indicate that the isomerization of the allyl group into the propenyl group was efficiently inhibited, while a number of uncharacterized peaks are observed due to the formation of partial propenyl groups when the polymerization of APSf was performed without the presence of hydroquinone (Figure 2.4).[13,45]

A series of functional membranes consisted of allyl polysulfone-graft-poly(dopamine methacrylamide) (AP-DM# membranes, where # indicates the feed ratio of APSf to dopamine methacrylamide(DMA)) was fabricated through

the following four steps: (1) preparing dope solutions by the polymerization of vinylic monomer moieties in APSf and DMA (*grafting-through* polymerization), (2) casting the resulting solutions as films onto PET non-woven fabric, (3) immersing the films for 24 h in a DI water bath for the formation of membranes by non-solvent induced phase separation (NIPS) method, and (4) immersing the membranes for 24 h in 0.25 M of sodium hydroxide (NaOH) aqueous solution (Figure 2.5). A clear and homogeneous solution containing allyl polysulfone-*graft*-poly(dopamine methacrylamide) in which poly(dopamine methacrylamide) (PDMA) brushes are grafted onto the APSf macromonomer can be prepared from step (1).[42,43] Commercial polysulfone (PSf) was included in the reaction mixture to improve stability of the membranes. Without the presence of commercial PSf, weak and fragile membrane was obtained mainly due to the poor mechanical property of the APSf caused by the low crystallinity (Figure 2.6).[46,47] For the preparation of PSf membrane, more dilute casting solution was used than for the preparation of AP-DM# membranes, because commercial polysulfone has larger molecular weight than APSf (50,000 g/mol and 5,300 g/mol for polysulfone and APSf, respectively). We could not handle the polysulfone solution of 0.7 mM or above concentration to fabricate the membrane because it is too viscous.

As shown in Table 2.1, the ratio of APSf to DMA was varied as 1:0.6, 1:0.8,

and 1:1 in order to investigate the effect of the content of DMA, and the resulting membrane was named as AP-DM0.6, AP-DM0.8, and AP-DM1 membranes, respectively. Free PDMA chains and residual DMA monomers were removed by immersing the membrane into NaOH solution.[45] ATR-IR spectra of the AP-DM# membranes exhibit the characteristic peaks ascribable to PSf and APSf at 2968 cm^{-1}, 1584 cm^{-1}, 1502 cm^{-1}, and 1487 cm^{-1}, correspond to aromatic -C-H and -C-C stretching of PSf and APSf (Figure 2.7). Comparing the APSf with the AP-DM# membranes, -C=C stretching frequency of allyl group at 1685 cm^{-1} disappeared after the polymerization, whereas peaks at 2849 cm^{-1} (C-C stretch) and 1659 cm^{-1} (C=O stretch) are newly observed in ATR-IR spectra of the AP-DM# membranes, verifying the incorporation of PDMA moieties. Nisin, a low molecular weight polypeptide antimicrobial substance (3,500 g/mol), was bonded onto the AP-DM# membranes through the Schiff base formation or Michael addition reaction between quinone group of the PDMA and N-terminal NH2 group of the nisin, as demonstrated in Figure 2.8.[45,48,49] In order to investigate the effect of nisin content on antifouling and antimicrobial properties, 1.0 g/L and 5.0 g/L of the nisin solution were used. The as-prepared nisin-immobilized membranes which used 1.0 g/L and 5.0 g/L of the nisin solution are referred to as AP-DM#-N1 and AP-DM#-N5 for short, respectively, when # indicates the feed ratio of DMA to APSf. Figure 2.9 shows a bonding density behavior of the AP-

DM#-N1 and AP-DM#-N5 membranes, obtained by measuring the weight change of the membranes as a function of immersion time to estimate the degree of nisin covalently immobilized on the AP-DM# membranes. Larger bonding density values were observed from the membranes containing larger PDMA contents. Moreover, the increase of the bonding density was observed with increasing the immersion time as expected, and the larger increase was also observed for AP-DM#-N5 membrane, treated with 5 g/L of nisin solution. The growth of bonding density was fast during the initial 6 h, and then the growth rate decreased and the bonding density value gradually approached to a constant value. Therefore, all membranes were immersed in the nisin solution for 6 h.

The incorporation of nisin was further confirmed by XPS analysis using AP-DM1, AP-DM1-N1, and AP-DM1-N5 membranes (Figure 2.10). Since the bonding density of AP-DM1 membrane more clearly increased than that of AP-DM0.8 and AP-DM0.6 membranes, AP-DM1, AP-DM1-N1, and AP-DM1-N5 membranes were analyzed in order to verify the presence of nisin on the membrane surface. The XPS C 1s core level spectrum of the AP-DM1 membrane was resolved into three peaks representing different chemical environments, revealing the presence of C-C, C-O, and C=O moieties observed at 285.5, 287.0, and 289.6 eV, respectively. In case of the C 1s spectra of the AP-DM1-N1 and AP-DM1-N5 membranes, new signals at 284.5 and 288.5 eV were found because of

the immobilization of nisin. The surface atomic compositions of the AP-DM1, AP-DM1-N1, and AP-DM1-N5 membranes were calculated in order to further investigate the presence of nisin on the membrane surface (Table 2.2). It was found that the nitrogen and sulfur content of the membranes increased after the immobilization of nisin because nisin contains larger content of nitrogen and sulfur.

Average pore diameter of the membranes is listed in Table 2.3. All AP-DM#-N1 and AP-DM#-N5 membranes demonstrate average pore diameter less than 50 nm, indicating that they can be used as UF membrane application. The larger pore diameter of AP-DM1 membrane than that of PSf membrane can be explained by the incorporation of the hydrophilic PDMA moiety in the AP-DM1 structure. The increase of the hydrophilicity of the polymer casting solution can increase the exchange rate of solvent (NMP) with non-solvent (DI water) during the NIPS process, then larger pore can be obtained.[48-50] Therefore, as the content of hydrophilic DMA increase, the average pore diameter increases from 16.8 nm (AP-DM0.6), 18.4 nm (AP-DM0.8), and 23.2 nm (AP-DM1). Meanwhile, it is also well known that the increase of the concentrations of the casting solution decreases the average pore diameter formed during the NIPS process because the solvent/non-solvent exchange rate decreases.[51,52] Since the concentration of casting solution for AP-DM0.6 and AP-DM0.8 membranes (0.7 mM and 0.8 mM,

respectively) is larger than that for PSf membrane (0.3 mM), smaller pores were observed for AP-DM0.6 and AP-DM0.8 membranes. When DMA content increases to the equivalent weight of PSf (or APSf), sufficient increase of the hydrophilicity of the casting solution can increase the exchange rate and then produce the larger pores.

The immobilization of the nisin into the membranes was found to decrease the average pore diameter, as reported by others; the average pore diameters of AP-DM#-N1 and AP-DM#-N5 membranes are always smaller than those of AP-DM# membranes and those of AP-DM#-N5 are also smaller than those of AP-DM#N1 membranes when they were prepared using the same amount of DMA.[53] However, SEM images (Figure 2.11, 2.12, and 2.13) of the membrane surface indicate that pores are not clogged by the nisin immobilization, showing reasonably high pure water flux values for AP-DM#-N1 and AP-DM#-N5 membranes as linsted in Table 2.3.

Porosity, thickness, and pure water permeability of PSf and AP-DM# membranes are listed in Table 2.3 to investigate the intrinsic properties of the membranes. It can be estimated from Table 2.3 that the porosity of the membranes increases with increasing the PDMA content in the casting solution because of the acceleration of exchange rate between solvent and non-solvent, as already mentioned for the average pore diameter. Additionally, porosity values of AP-

DM1, AP-DM0.8, and AP-DM0.6 membranes decrease by the increase of the nisin content on the membrane, indicating that the immobilization of the nisin induces the decrease of the porosity as well as the average pore diameter. Porosity value of the PSf membrane shows a minor difference compared to that of the AP-DM1, AP-DM0.8, and AP-DM0.6 membranes, because all membranes have a typical asymmetric structure composed of dense skin layer and porous sublayer. The thickness of the membranes wer found to be quite close, because all membranes were casted using a doctor blade having the same thickness. Pure water permeability of AP-DM0.6, AP-DM0.8, AP-DM1 membranes is 780.6, 1634.1, and 2848.1 LMH, respectively, while that of PSf membrane is 883.6 LMH, clearly verifying that the presence of hydrophilic PDMA could induce the enhancement of the filtration performance by stimulate the transport of water molecules in the membrane.[13] In the same vein, although the average pore diameter of the AP-DM0.8 membrane is smaller than that of the PSf membrane, larger pure water permeability of the AP-DM0.8 membrane was observed.

Figure 2.14 shows surface and cross-sectional morphologies of the membranes investigated by FE-SEM measurements. For all membranes, asymmetric structure composed of a dense top layer and a porous sublayer was observed.[46,47,50] Since the molecular weight of nisin is small enough to be immobilized with minimizing the pore blocking, there is no significant morphological difference

among AP-DM#, AP-DM#-N1, and AP-DM#-N5 membranes (Figure 2.11, 2.12, and 2.13).

It is well-known that the hydrophilicity of membrane surface is the predominant reason for antifouling behavior because foulants easily adsorb on membrane surface and/or inner pores when the membrane surface is hydrophobic. The hydrophilicity of the AP-DM#-N1 and AP-DM#-N5 membranes was carried out by measuring air captive bubble contact angles on the membranes equilibrated in deionized (DI) water (Figure 2.15). The pristine PSf membrane demonstrates the largest contact angle value among the membranes due to its hydrophobic nature. As shown in Figure 2.15(a), the contact angle values of the AP-DM# membranes are smaller than that of the PSf membrane based on the presence of hydrophilic PDMA moieties on the surface. The contact angle values of the AP-DM0.6, AP-DM0.8, and AP-DM1 membranes were 56.1˚ ± 1.9˚, 50.0˚ ± 1.3˚, and 37.9˚ ± 1.1˚, respectively, indicating that an increase in the PDMA content improve the hydrophilicity of the AP-DM# membranes. For all AP-DM#-N1 and AP-DM#-N5 membranes, the contact angle increases due to the incorporation of nisin, implying the decreased hydrophilicity of the membrane. However, it was clearly observed that the all AP-DM#-N1 and AP-DM#-N5 membranes still have more hydrophilic surface than the pristine PSf membrane.[17,54]

Dead-end filtration tests were performed to investigate the fouling resistance

and flux recovery ability of the membranes using bovine serum albumin (BSA) as a model foulant. Normalized flux variations and flux recovery abilities of the membranes are shown in Figure 2.16. As shown in Figure 2.16(a), the pristine PSf membrane showed significant flux decrease at the initial filtration stage, and about 40% flux decline was observed after 60 min during BSA solution filtration. Low fouling resistance of the PSf membrane is attributed from the hydrophobic surface where the foulants are prone to adsorb, as reported by us and others.[5,6,10-13] Meanwhile, much larger flux values were observed in the AP-DM0.6-N1, AP-DM-0.8-N1, and AP-DM1-N1 membranes. The AP-DM-0.8-N1 membrane was found to be more effective for reducing fouling than the AP-DM0.6-N1 membrane. After 60 min of dead-end filtration, the flux-decline ratio (*DR*) of the AP-DM-0.8-N1 membrane (21.6%) was smaller than that of the AP-DM0.6-N1 membrane (23.5%). AP-DM1-N1 membrane bearing the high content of PDMA moieties exhibited the smallest *DR* value (20.9%) among the membranes, as shown in Figure 2.17. It was clearly observed that the AP-DM# membranes with higher contents of PDMA moieties have better antifouling properties against foulants. The dopamine moiety has been already known as an effective coating material for preventing the adsorption of foulants because the hydrogen bonding between catechol groups in PDA and water molecules can provide an energetic and steric-entropic barrier against the adhesion of foulants to the membrane surface in an

aqueous environment.[17,30,31,51,52] The increase in the PDMA content in the membranes could also enhance the hydrophilicity of the membrane surfaces, resulting in improving the fouling resistance of the membrane, as reported by us.[17] Meanwhile, the AP-DM1-N1 and AP-DM1-N5 membrane exhibited low protein rejection (less than 50%), while the PSf, AP-DM0.6-N1, AP-DM0.6-N5, AP-DM-0.8-N1, AP-DM-0.8-N5 membranes properly reject the protein (more than 97%). Therefore, AP-DM0.6 or AP-DM0.8 membranes could be used as the UF membrane, exhibiting noticeable fouling resistance with removing the protein in the feed stream. Since there is an electrostatic interaction between the cationic peptide nisin and the negatively charged BSA protein, the AP-DM1-N5 membrane having higher nisin content exhibits relatively larger flux decline (24.4%) than the AP-DM1-N1 membrane, as described in Figure 2.17. Nevertheless, it is clear that both AP-DM1-N1 and AP-DM1-N5 membranes have superior fouling resistance compared to the pristine PSf membrane.

At 60 min after initial feed of the BSA solution, the membranes were washed with DI water, after which the water flux of the cleaned membranes was measured again. Flux recovery ability of the membranes was evaluated by calculating flux recovery ratio (*FRR*), as demonstrated in Figure 2.17. As expected, *FRR* value of the AP-DM# membranes are larger than that of the pristine PSf membrane, originated from low interacting force between the PDMA moieties and the protein,

as already measured and reported by us.[17,25] The FRR value was found to increase with the increase of the DMA feed amount and the decrease of the nisin content, as expected from the flux decline behavior. Considering the above results on fouling resistance and flux recovery of the AP-DM# membranes, we can conclude that the presence of hydrophilic PDMA on the membrane surface is essential to improving the fouling resistance of membranes.

In order to maintain filtration performance of membrane in industrial applications, the antimicrobial property is important in addition to the fouling resistance. It has been reported that bacteria attached to membranes can produce a biofilm causing membrane flux decline when the population of the bacterial on the membrane is larger than a certain concentration, known as the quorum sensing effect.[17,57] The antimicrobial properties of the membranes were carried out against model Gram-positive (*S. aureus*, ATCC 6537) bacteria by a shaking flask method to confirm the antimicrobial effect of the nisin content in the membrane surfaces. Figure 2.18 demonstrates the result of antimicrobial tests of PSf, AP-DM#-N1, and AP-DM#-N5 membranes and the bacterial inhibition rate against S. aureus was obtained by calculating Equation(2.5). As shown in the figure, a large amount of S. aureus was found on the surface of pristine PSf membrane, as already reported.[17] The AP-DM0.6-N5, AP-DM-0.8-N5, and AP-DM1-N5 membranes exhibited excellent antimicrobial activity, with bacterial inhibition

rates higher than 85% (85.9, 89.7, and 92.6% for AP-DM0.6-N5, AP-DM-0.8-N5, and AP-DM1-N5, respectively), whereas the AP-DM1-N1 membrane showed a slightly low bacterial inhibition rate of about 83.5%. The increase in nisin content on the membrane surface induces the increase of antimicrobial properties of the AP-DM# membranes, because of robust antimicrobial property of nisin.[21,45] AP-DM0.6-N1 and AP-DM-0.8-N1 membranes exhibited much low bacterial inhibition rate of about 7.5% and 34.0%, due to their scarce presence of nisin on the membrane surfaces. As expected, the antimicrobial properties of the AP-DM# membranes increase with the increase of nisin content. Since the bacterial inhibition rate of the AP-DM0.6-N5 membrane is larger than that of the AP-DM1-N1 membrane, it is reasonable to conclude that the antimicrobial property is mainly determined by the concentration of nisin solution during the immobilization step, rather than the amount of PDMA moiety on the membrane surface.

2.4. Conclusion

Membranes containing allyl polysulfone-*graft*-poly(dopamine methacrylamide) were prepared by grafting-through polymerization and subsequent NIPS method without cumbersome purification steps of the polymer. Antimicrobial nisin was covalently bonded on the as-prepared membrane surface by the reaction between the catechol group in PDMA and the nisin. The AP-DM#-N1 and AP-DM#-N5 membranes exhibited the antifouling and antimicrobial property, compared with the bare PSf membrane. Especially, The AP-DM0.8-N5 membrane demonstrated noticeable antimicrobial property with a small deterioration of the filtration performance based on the proper composition of APSf, DMA, and nisin. We believe that this work provides a deep understanding of a new way to fabricate membrane materials with various functional properties for a range of applications.

2.5. References

[1] Miller DJ, Paul DR, Freeman BD. Polymer 55 (2014) 1375-1383.

[2] Zhao S, Wang Z, Qiao ZH, Wei X, Zhang CX, Wang JX, Wang SC. J Mater Chem A 1 (2013) 246-249.

[3] Vandezande P, Gevers LEM, Vankelecom IF, J Chem Soc Rev 37 (2008) 365-372.

[4] Shannon MA, Bohn PW, Elimelech M, Georgiadis JG, Marinas BJ, Mayes AM. Nature 452 (2007) 301-310.

[5] Guo W, Ngo HH, Li J. Bioresour Technol 122 (2012) 27-34.

[6] Lim AL, Bai R. J Mater Sci 216 (2003) 279-290.

[7] Kim D-G, Kang H, Han S, Lee J-C. J Mater Chem 22 (2012) 8654-8661.

[8] Kim D-G, Kang H, Han S, Kim HJ, Lee J-C. RSC Adv 3 (2013) 18071-18081.

[9] Kim D-G, Kang H, Han S, Lee J-C. ACS Appl Mater Interfaces 4 (2012) 5898-5906.

[10] Ng LY, Mohammad AW, Leo CP, Hilal N. Desalination 308 (2013) 15-33.

[11] Zhao Y-F, Zhu L-P, Jiang J-H, Yi Z, Zhu B-K, Xu Y-Y. Ind Eng Chem Res 53 (2014) 13952-13962.

[12] Cai T, Yang WJ, Neoh KG, Kang ET. Ind Eng Chem Res 51 (2012) 15962-

15973.

[13] Chem Y, Ying L, Yu W, Kang ET, Neoh KG. Macromolecules 36 (2003) 9451-9457.

[14] Huang X, Wang W, Liu Y, Wang H, Zhang Z, Fan W, Li L. Chem Eng J 273 (2015) 421-429.

[15] Qin JJ, Cao YM, Li YQ, Li Y, Oo MH, Lee H. Sep Purif Technol 36 (2004) 149-155.

[16] Li X, Cai T, Chung T-S. Environ Sci Technol 48 (2014) 9898-9907.

[17] Choi Y-S, Kang H, Kim D-G, Cha S-H, Lee J-C. ACS Appl Mater Interfaces 6 (2014) 21297-21307.

[18] McCloskey BD, Park HB, Rowe BW, Miller DJ, Chun BJ, Kin K, Freeman BD. Polymer 51 (2010) 3472-3485.

[19] Ham HO, Liu Z, Lau KHA, Lee H, Messersmith PB. Angew Chem Int Ed 50 (2011) 732-736.

[20] Faure E, Lecomte P, Lenoir S, Vreuls C, Van De Weerdt C, Archambeau C, Martial J, Jerome C, Duwez A-S, Detrembleur C. J Mater Chem 21 (2011) 7901-7904.

[21] Alves D, Pereira MO. Biofouling 30 (2014) 483-499.

[22] Cho WM, Joshi BP, Cho H, Lee KH. Bioorg Med Chem Lett 17 (2007) 5772-5776.

[23] Gao G, Yu K, Kindrachuk J, Brooks DE, Hancock REW, Kizhakkedathu JN. Biomacromolecules 12 (2011) 3715-3727.

[24] Kim HJ, Kim D-G, Yoon H, Choi Y-S, Yoon J, Lee J-C. Adv Mater Interfaces 2 (2015) 1500298.

[25] Shi Q, Su Y, Zhu S, Li C, Zhao Y, Jiang Z. J Membr Sci 303 (2007) 204-212.

[26] Asatekin A, Kang S, Elimelech M, Mayes AM, J Membr Sci 298 (2007) 36-146.

[27] Rahimpour A, Madaeni SS. J Membr Sci 305 (2007) 299-312.

[28] Zhou Z, Rajabzadeh S, Shaikh AR, Kakihana Y, Ma W, Matsuyama H. J Membr Sci 514 (2016) 537-546.

[29] Zhao X, Su Y, Cao J, Li Y, Zhang R, Liu Y, Jiang Z. J Mater Chem A 3 (2015) 7287-7295.

[30] Li YS, Yan L, Xiang CB, Hong LJ. Desalination 196 (2006) 76-83.

[31] Wu H, Mansouri J, Chen V. J Membr Sci 433 (2013) 135-151.

[32] Huang Z-Q, Zheng F, Zhang Z, Xu H-T, Zhou K-M. Desalination 292 (2012) 64-72.

[33] Cheng C, He A, Nie C, Xia Y, He C, Ma L, Zhao C. J Mater Chem B 3 (2015) 4170-4180.

[34] Zhang P-Y, Xu Z-L, Yang H, Wei Y-M, Wu W-Z. Chem Eng Sci 97 (2013)

296-308.

[35] Feng S, Shang Y, Wang S, Xie X, Wang Y, Wang Y, Xu J. J Membr Sci 346 (2010) 105-112.

[36] Zhang R, Su Y, Peng J, Fan X, Jiang Z, Zhao X, Liu J, Li Y, Zhao J. Polymer 55 (2013) 1347-1357.

[37] Tao M, Liu F, Xue L. J Mater Chem 22 (2012) 9131-9137.

[38] Zhang P-Y, Xu Z-L, Yang H, Wei Y-M, Wu W-Z. Chem Eng Sci 97 (2013) 296-308.

[39] Qin H, Sun C, He C, Wang D, Cheng C, Nie S, Sun S, Zhao C. J Membr Sci 468 (2014) 172-183.

[40] Tsukahara Y, Tsutsumi K, Yamashita Y, Shimada S. Macromolecules 23 (1990) 5201-5208.

[41] Cho HY, Krys P, Szcześniak K, Schroeder H, Park S, Jurga S, Buback M, Matyjaszewski K. Macromolecules 48 (2015) 6385-6395.

[42] Gieseler D, Jordan R. Polym Chem 6 (2015) 4678-4689.

[43] Hadasha W, Klumperman B. Polym Int 63 (2014) 824-834.

[44] Sahoo BB, Raj TT, Srinvasarao AR, Lens JP Monomers for the preparation of silylated polycarbonate polymers. PCT Int. Appl. WO2008079358, 2008.

[45] Ni J, Zhao C, Zhang G, Zhang Y, Wang J, Ma W, Liu Z, Na H. Chem

Commun 47 (2011) 8943-8945.

[46] Ko T, Kim K, Jung B-K, Cha S-H, Kim S-K, Lee J-C. Macromolecules 48 (2015) 1104-1114.

[47] Villa DC, Angioni S, Barco SD, Mustarelli P, Quartarone E. Adv Energy Mater 4 (2014) 1301949-1301956.

[48] Yu L, Zhang Y, Zhang B, Liu J, Zhang H, Song C. J Membr Sci 447 (2013) 452-462.

[49] Zhao H, Wu L, Zhou Z, Zhang L, Chen H. Phys Chem Chem Phys 15 (2013) 9084-9092.

[50] Lee J, Chae H-R, Won YJ, Le K, Lee C-H, Lee HH, Kim I-C, Lee J-M. J Membr Sci 448 (2013) 223-230.

[51] Cheryan M Ultrafiltration and microfiltration handbook; CRC Press: Lancaster, USA, 1998.

[52] Strathmann H, Kock K. Desalination 21 (1977) 241-255.

[53] Swan EEL, Popat KC, Desai TA. Biomaterials 26 (2005) 1969-1976.

[54] Sigal GB, Mrksich M, Whitesides GM. J Am Chem Soc 120 (1998) 3464-3473.

[55] Hezberg M, Elimelech M. J Membr Sci 295 (2007) 11-20.

[56] Parsek MR, Greenberg EP. Trends Microbiol 13 (2005) 27-33.

[57] Chem X, Zhang G, Zhang Q, Zhan X, Chen F. Ind Eng Chem Res 54

(2015) 3813-3820.

Table 2.1. Preparation of the membranes.

Sample	Macromonomer	Monomer	Initiator	Matrix	Solvent	Solid Concentration[a]	Nisin concentration
	APSf (g)	DMA (g)	AIBN (g)	PSf (g)	NMP (mL)	(mM)	(g/L)
PSf	0	0	0	2.0	14.4	0.3	0
AP-DM0.6	1.0	0.6	0.08	1.0	10.3	0.7	0
AP-DM0.6-N1	1.0	0.6	0.08	1.0	10.3	0.7	1.0
AP-DM0.6-N5	1.0	0.6	0.08	1.0	10.3	0.7	5.0
AP-DM0.8	1.0	0.8	0.09	1.0	10.3	0.8	0
AP-DM-0.8-N1	1.0	0.8	0.09	1.0	10.3	0.8	1.0
AP-DM-0.8-N5	1.0	0.8	0.09	1.0	10.3	0.8	5.0
AP-DM1	1.0	1.0	0.10	1.0	10.3	0.9	0
AP-DM1-N1	1.0	1.0	0.10	1.0	10.3	0.9	1.0
AP-DM1-N5	1.0	1.0	0.10	1.0	10.3	0.9	5.0

[a] Solid concentration was obtained by dividing the sum of the weight of solid content (APSf, DMA, AIBN, and PSf) by the volume of NMP.

Table 2.2. XPS elemental compositon (in at%) of the surfaces of AP-DM1, AP-DM1-N1, and AP-DM1-N5 membranes.

	C 1s	O 1s	N 1s	S 2p
AP-DM1	76.07	16.48	6.83	0.62
AP-DM1-N1	71.80	20.37	7.05	0.78
AP-DM1-N5	66.92	21.99	9.86	1.24

Table 2.3. Intrinsic properties of the membranes.

Sample	Porosity (%)	Average pore diameter (nm)	Thickness (μm)	Pure water permeability (LMH)
PSf	75.9 ± 2.5	19.7	209.3 ± 2.8	883.6 ± 12.8
AP-DM0.6	73.6 ± 0.9	16.8	228.6 ± 3.5	780.6 ± 25.5
AP-DM0.6-N1	56.8 ± 0.3	16.7	233.6 ± 5.4	767.1 ± 12.3
AP-DM0.6-N5	49.7 ± 1.9	16.4	217.4 ± 2.3	771.4 ± 9.4
AP-DM0.8	76.3 ± 0.6	18.4	235.9 ± 4.5	16342.1 ± 12.7
AP-DM-0.8-N1	60.8 ± 2.2	14.0	224.3 ± 9.6	1196.3 ± 5.4
AP-DM-0.8-N5	54.3 ± 5.1	13.1	223.6 ± 12.9	827.5 ± 11.3
AP-DM1	78.7 ± 0.8	23.2	218.6 ± 3.2	2848.1 ± 28.7
AP-DM1-N1	66.9 ± 5.8	22.3	208.9 ± 8.6	2378.0 ± 36.1
AP-DM1-N5	64.9 ± 3.1	20.1	199.7 ± 9.6	1817.6 ± 15.1

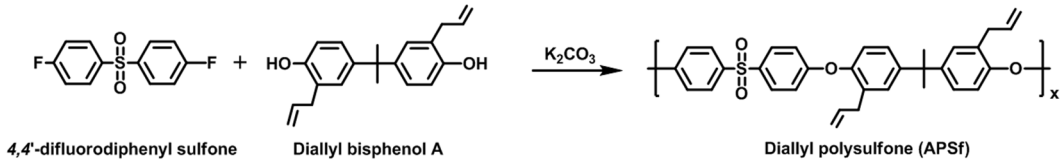

Figure 2.1. Synthesis of allyl polysulfone (APSf).

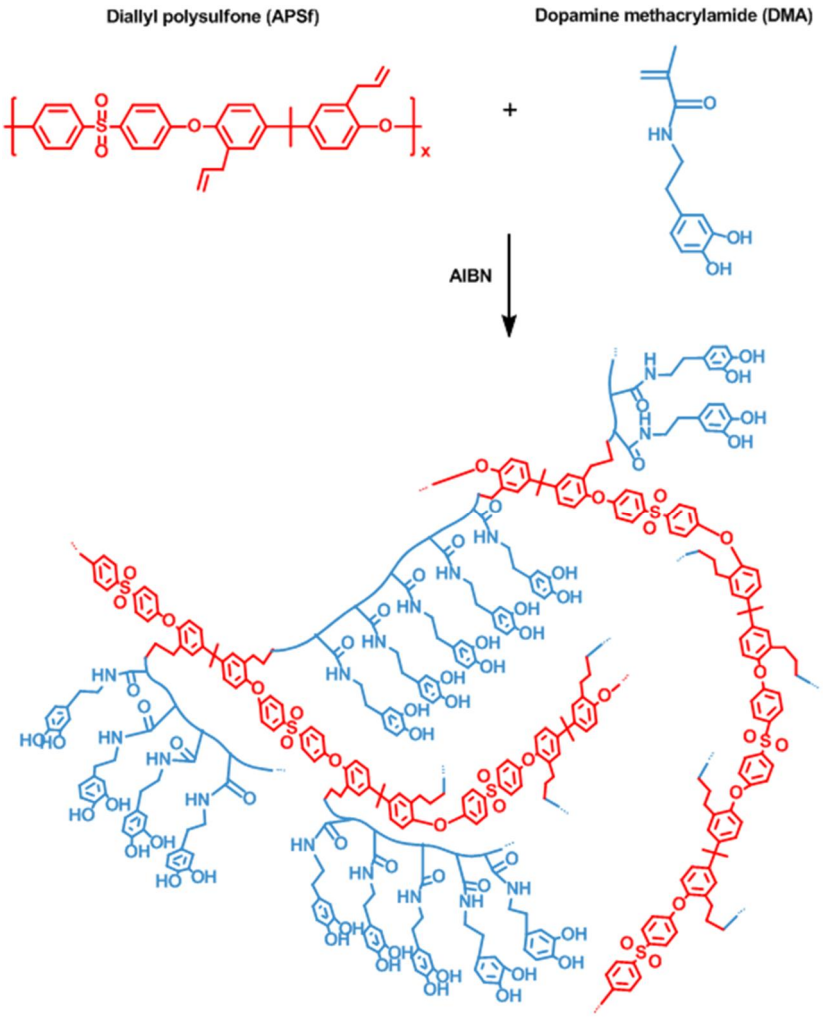

Figure 2.2. Synthesis of allyl polysulfone-*graft*-poly(dopamine methacrylamide).

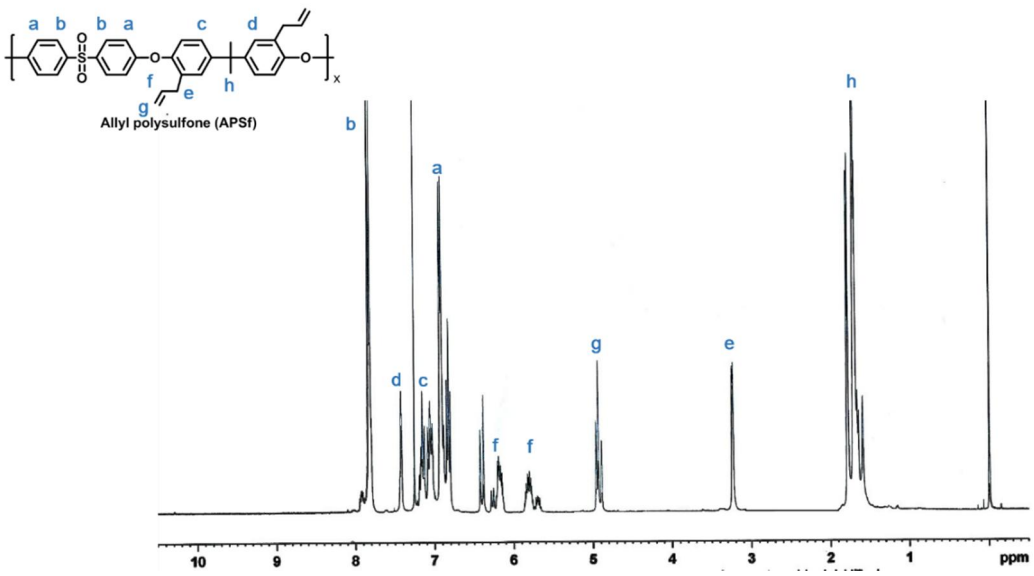

Figure 2.3. ^{1}H NMR spectra of allyl polysulfone (APSf) synthesized in the presence of hydroquinone (HQ).

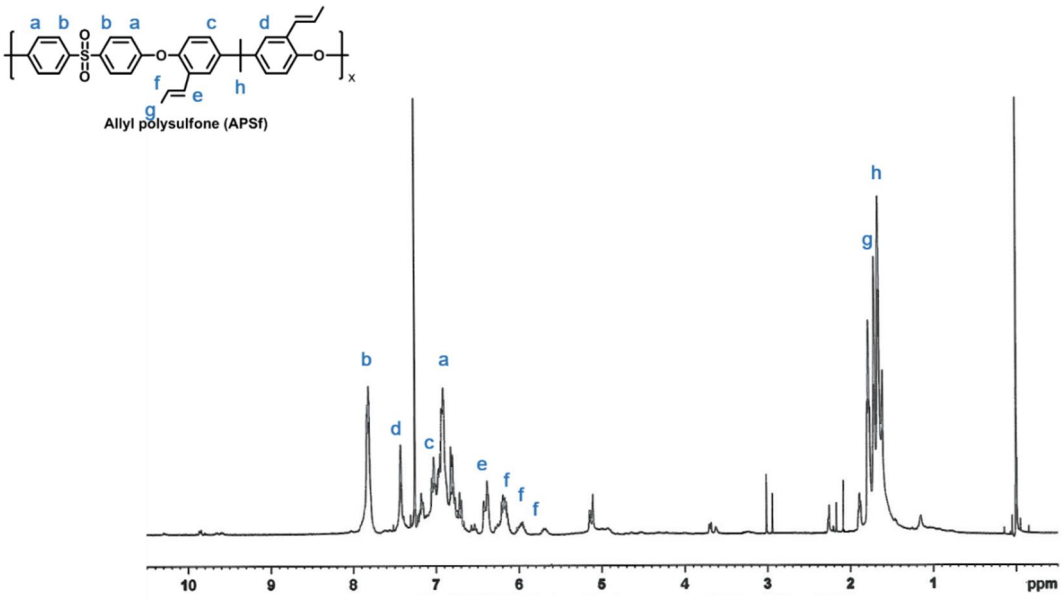

Figure 2.4. ^{1}H NMR spectra of allyl polysulfone synthesized without the presence of hydroquinone.

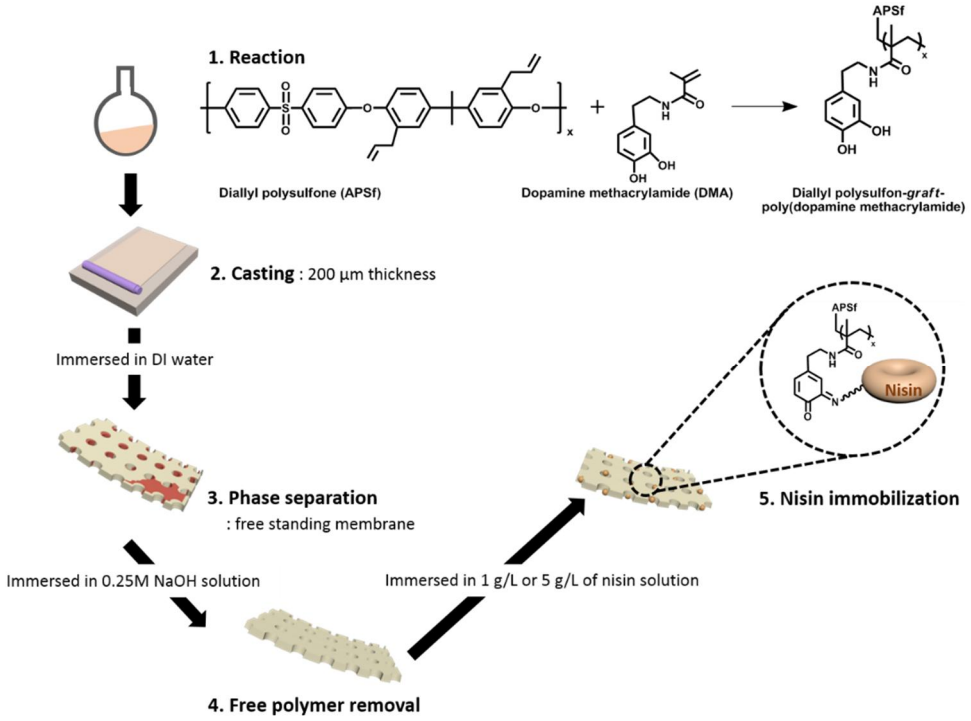

Figure 2.5. Preparation of the AP-DM#-N1 and AP-DM#-N5 membranes.

Figure 2.6. Photograph of AP-DM1 membrane prepared without the presence of PSf matrix.

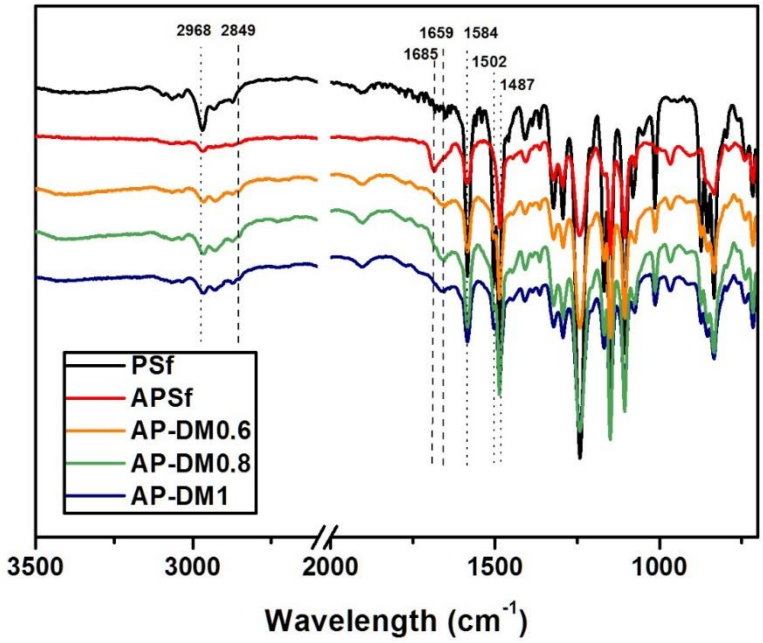

Figure 2.7. ATR-FTIR spectra of polysulfone (PSf) membrane and the functionalized membranes fabricated using the as-prepared casting solution containing allyl polysulfone-graft-poly(dopamine methacrylamide) (AP-DM# membranes, where # indicates feed ratio of dopamine methacrylamide to APSf).

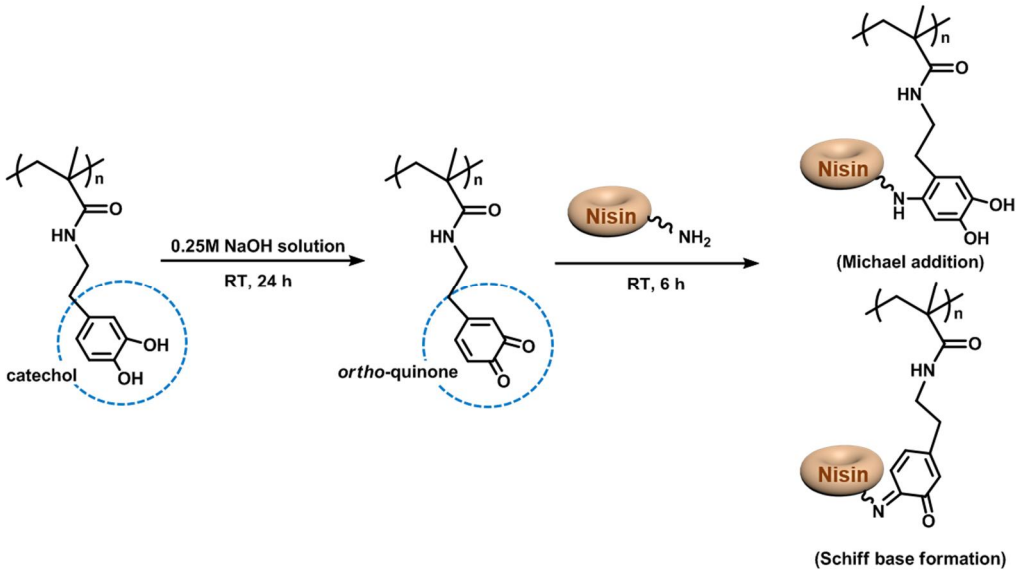

Figure 2.8. Reaction between PDMA and nisin.

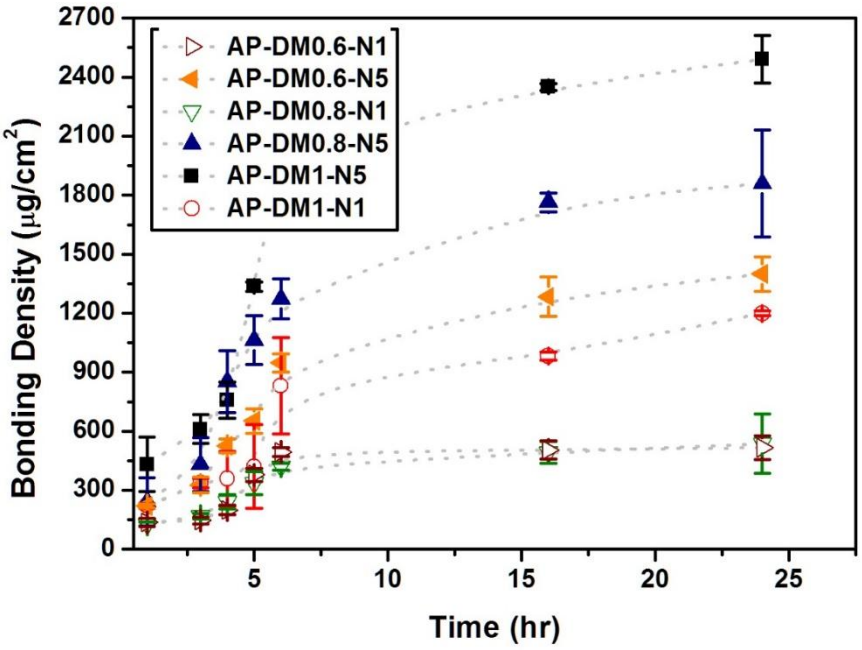

Figure 2.9. Variations of bonding density for nisin on the AP-DM#-N1 and AP-DM#-N5 membranes as a function of immersion time.

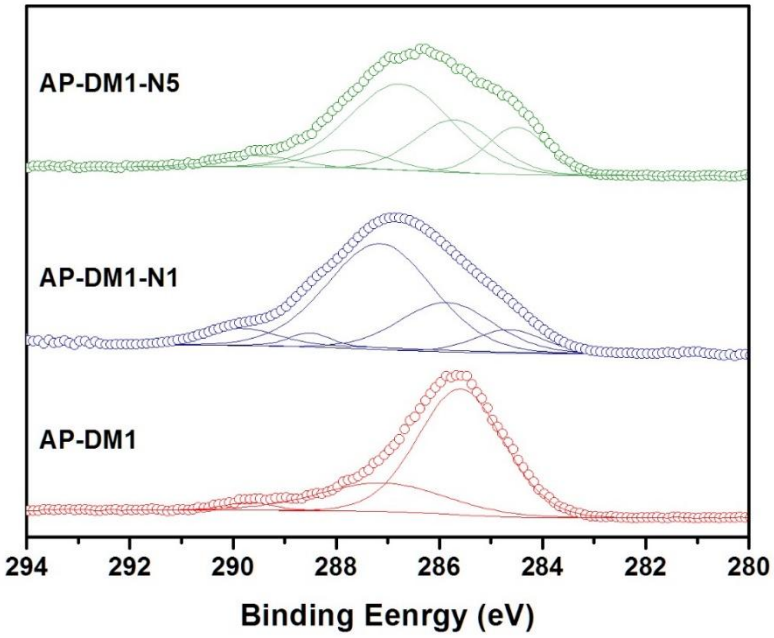

Figure 2.10. XPS C 1s core level spectra of the surfaces of AP-DM1, AP-DM1-N1, and AP-DM1-N5 membranes.

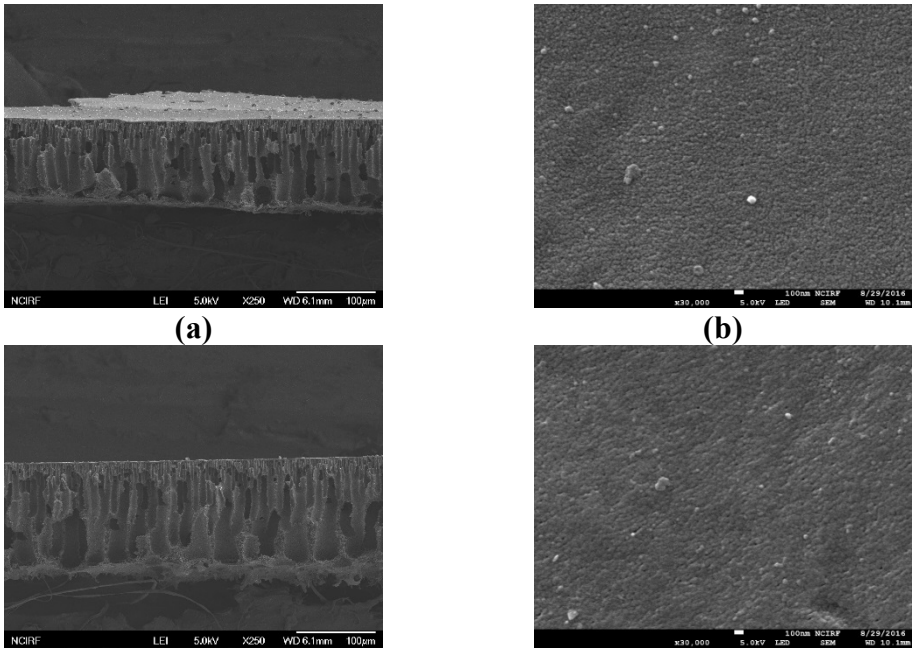

(a) **(b)**

(c) **(d)**

Figure 2.11. FE-SEM micrographs of (a,b) AP-DM0.6-N1 and (c,d) AP-DM0.6-N5 membranes.

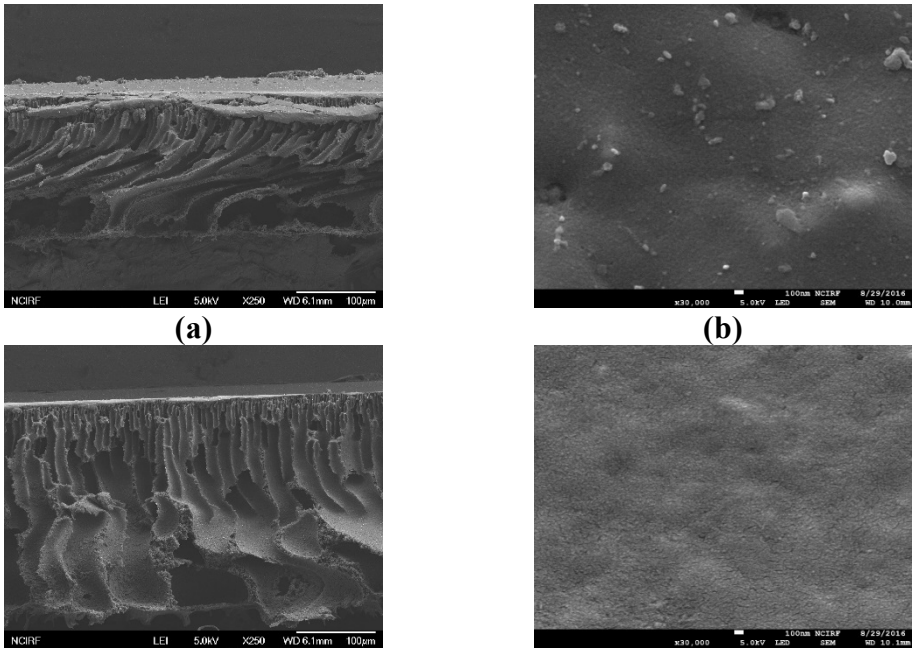

Figure 2.12. FE-SEM micrographs of (a,b) AP-DM0.8-N1 and (c,d) AP-DM0.8-N5 membranes.

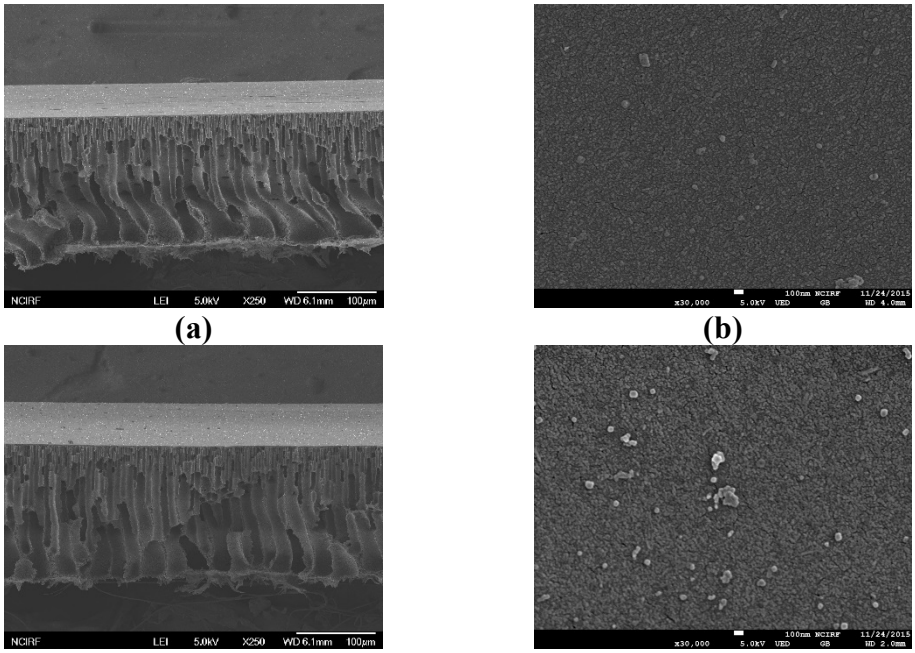

(a) **(b)**

(c) **(d)**

Figure 2.13. FE-SEM micrographs of (a,b) AP-DM1-N1 and (c,d) AP-DM1-N5 membranes.

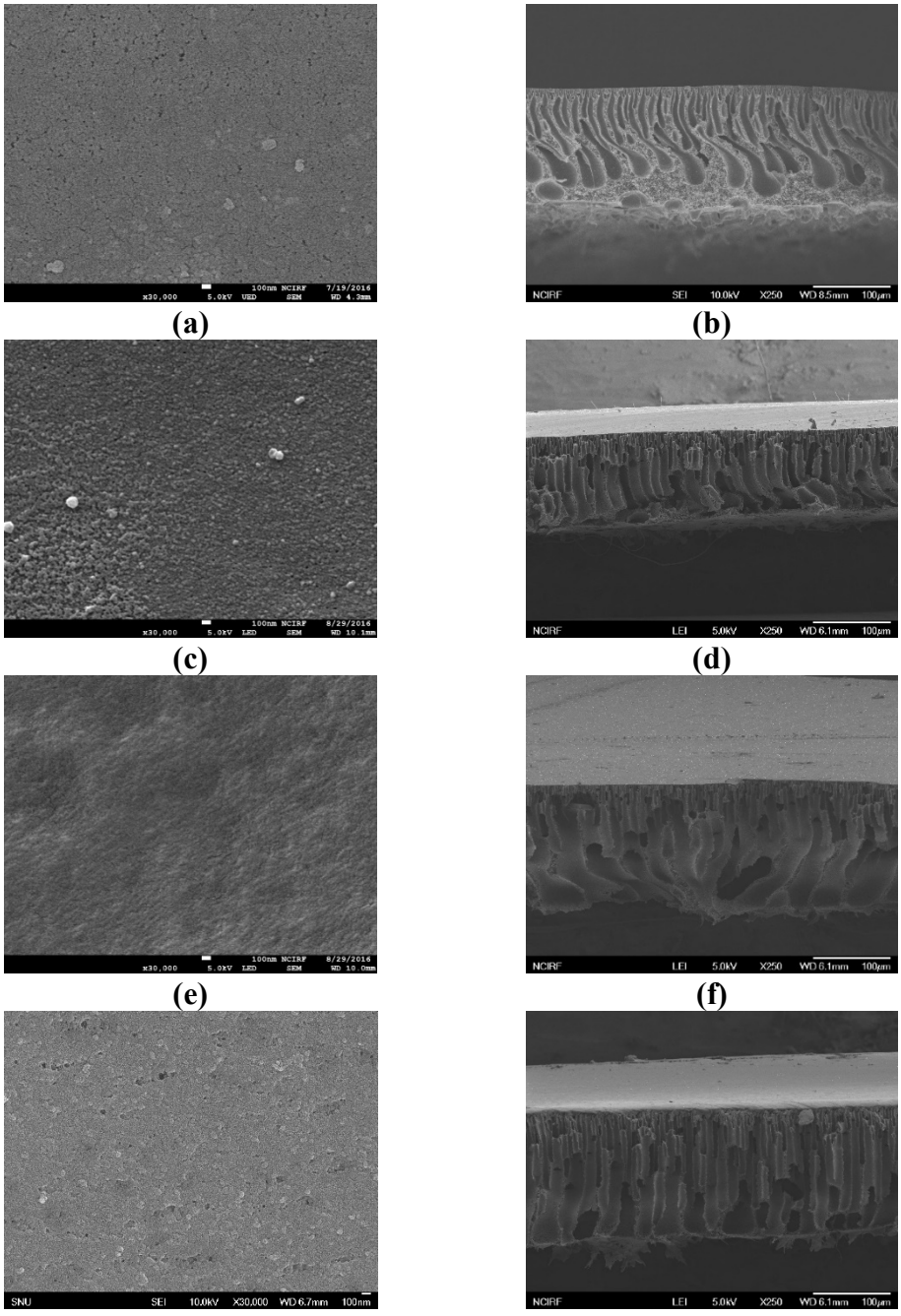

Figure 2.14 FE-SEM micrographs of (a,b) PSf, (c,d) AP-DM0.6, (e,f) AP-DM0.8, and (g,h) AP-DM1 membranes.

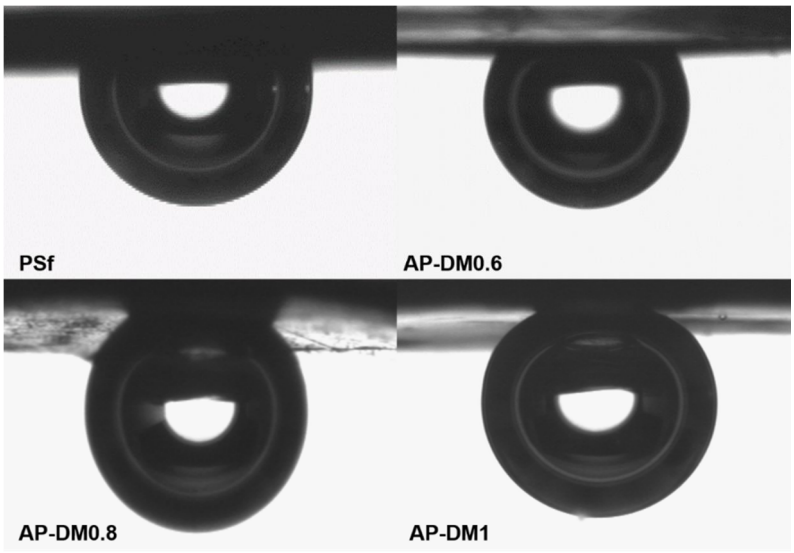

(a)

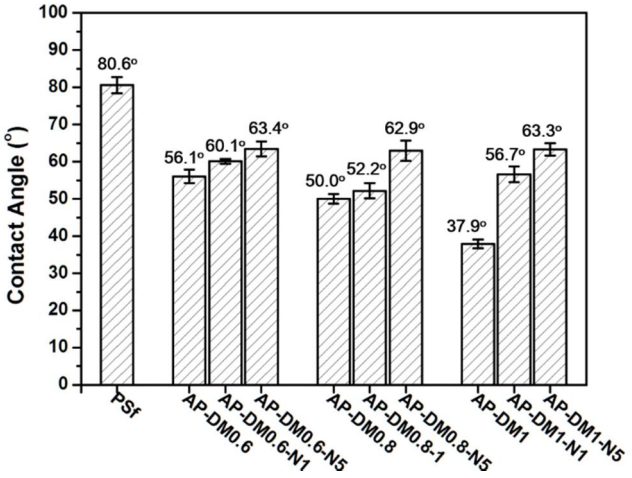

(b)

Figure 2.15 (a) Air captive bubble contact angle images of PSf, AP-DM0.6, AP-DM0.8, and AP-DM1 membranes (b) air captive bubble contact angle values of APSf, a series of AP-DM#-N1 and AP-DM#-N5 membranes.

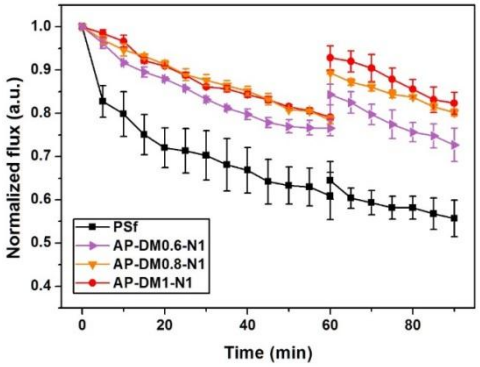

(a)

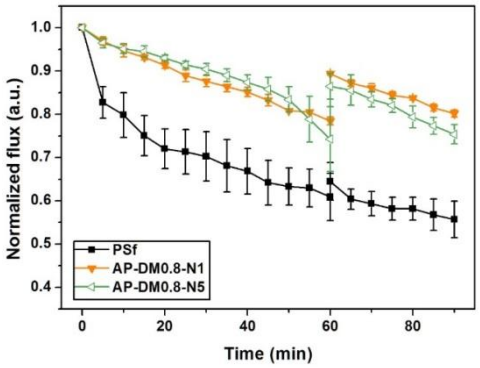

(b)

Figure 2.16 Time dependence of water flux variations during the BSA solution filtration: (a) flux behavior of PSf, AP-DM0.6-N1, AP-DM-0.8-N1, and AP-DM1-N1 membranes (b) flux behavior of PSf, AP-DM0.8-N1, and AP-DM0.8-N5 membranes. After 60 min of the initial filtration, all membranes were washed with deionized (DI) water and water flux values were measured subsequently.

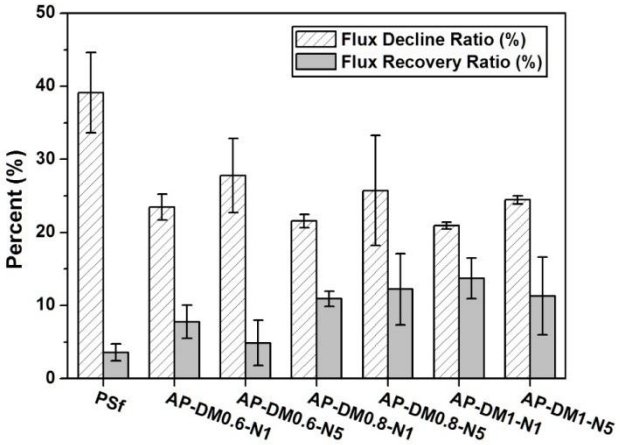

Figure 2.17 Flux decline ratio (*DR*) and flux recovery ratio (*FRR*) of the membranes.

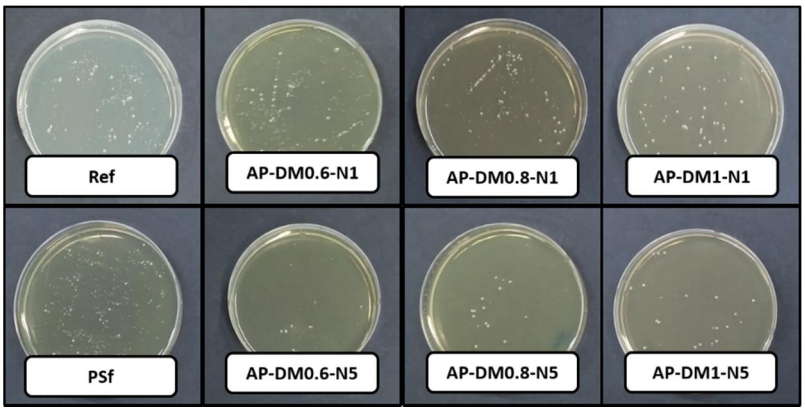

(a)

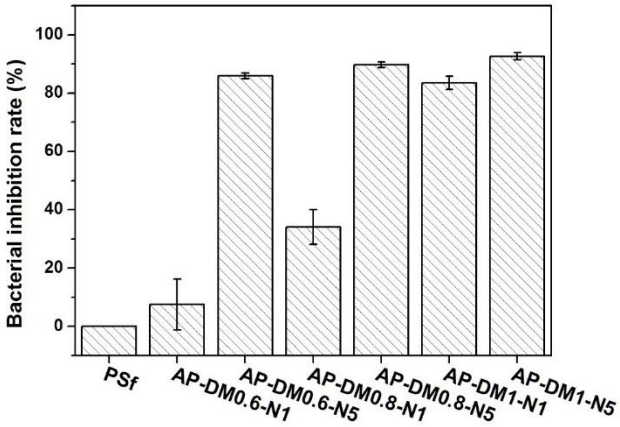

(b)

Figure 2.18 Results of antimicrobial test of the blank sample, PSf membrane, AP-DM#-N1 membrane, AP-DM#-N5 membrane: (a) Photographic results and (b) bacterial inhibition rates.

Chapter 3

Thin Film Composite (TFC) Membranes for Forward Osmosis (FO) Application

3.1. Introduction

Water shortage and resource depletion has become major concerns for the sustainable future of humanity.[1-3] Membrane technologies have been regarded as the most effective strategies to address global water quality and scarcity issues.[4,5] Forward osmosis (FO), one of membrane-based separation process, is an attractive alternative technology compared to conventional pressure-driven process for water treatment.[6,7] In FO system, the osmotic pressure gradient generated by a feed solution and a draw solution induce the diffusion of water molecules across the semi-permeable membrane. The absence of external hydraulic pressure in FO process significantly reduce the overall energy consumption, high rejections to a wide range of contaminants, and low membrane fouling propensity.[8-10]

FO membranes should possess semipermeable nature that facilitate water diffusion while rejecting other components.[11] Most FO membranes are designed to have an asymmetric structure composed of a thin polyamide selective layer on top of a porous substrate, which is a predominant structure of thin-film composite (TFC) reverse osmosis (RO) membrane. The TFC RO membranes include thick porous substrates in order to withstand extremely high hydraulic pressures during

the RO process. Therefore, application of the RO membrane in the FO system cause severe internal concentration polarization (ICP), defined as the decrease in solute concentration at the transverse boundaries of porous substrate.[12,13]

Much attention has been focused on the mitigation of ICP such as (1) reducing the thickness of substrate,[14,15] (2) fabricating the substrate with desirable porous morphology,[15,16] and (3) altering the physiochemical properties of substrate enhancing the hydrophilicity.[16,17] Among them, The improvement of substrate hydrophilicity has been known as an effective strategy to reduce the ICP, because a relatively hydrophilic substrate is easily wetted in water and ensures effective water transport, while vapor or air trapped in the pores exacerbates ICP within the hydrophobic substrate.[18]

Herein, we prepared TFC membranes having novel hydrophilic substrate bearing zwitterionic poly(sulfobetaine methacrylate) (PSBMA) for FO application. The surface properties, permeation properties, FO performances, and fouling resistance of the membranes were carried out and compared to those of bare TFC membrane having hydrophobic substrate.

3.2. Experimental

Materials

2,2'-Diallylbisphenol A (DBPA, 85.0%) was purchased from Sigma-Aldrich Co., LLC. and purified by the procedure reported before.[19] 1,3-propane sultone (98.0%) and 1,3,5-benzenetricarbonyl trichloride (TMC, 98.0%) were also purchased from Sigma-Aldrich Co., LLC. and used as received. m-phenylenediamine (MPD, 98.0%) was purchased from Alfa Aesar Co. Ltd. and used without further purification. 4,4'-Difluorodiphenyl sulfone (DFDPS, 99.0%) was obtained from Tokyo Chemical Industry Co., Ltd. and recrystallized from toluene prior to use. Dimethylaminoethyl methacrylate (DMAEMA) was purchased from Sigma-Aldrich Co., LLC. and passed through a column filled with alumina to remove the inhibitor prior to use. 2,2'-Azobis(isobutyronitrile) (AIBN) was purchased from Junsei Chemical Co., Ltd. and purified by recrystallization from ethanol. *N*-Methyl-2-pyrrolidone (NMP, 99.0%) and toluene (99.0%) were purchased from Junsei Chemical Co., Ltd. and dried over a molecular sieve (4Å). Ethyl acetate (98.0%) and Methanol (99.0%) were obtained from Daejung Chemicals & Metals Co., Ltd. Polysulfone (PSf, Udel® P-1700) was kindly supplied by Solvay Advanced Polymers. A polyester non-woven fabric (PET,

Grade A3249) was purchased from Ahlstrom Co. Ltd. in order to use as a backing layer for the porous substrate. Deionized (DI) water was obtained from water purification system (Synergy, Millipore, USA), having a resistivity of 18.3MΩ cm. Bacto agar and Difco tryptic soy broth were obtained from Becton, Dickinson and Co. (BD). All other reagents and solvents were used as received.

Synthesis of allyl polysulfone (APSf) macromonomer.

Allyl polysulfone (APSf) was synthesized by the condensation polymerization of DBPA with DFDPS, as shown in Scheme 1.[20] A 250 mL three neck round bottom flask equipped with an overhead mechanical stirrer, a Dean-Stark trap, and nitrogen inlet and outlet was charged with DBPA (3.08 g, 10 mmol), DFDPS (2.54 g, 10 mmol), K_2CO_3 (1.52 g, 11 mmol), and hydroquinone (0.011 g, 0.1 mmol) in 6 mL of NMP. Then 3mL of toluene (NMP/toluene = 2/1 v/v) was added as an azeotropic agent. The reaction mixture was refluxed at 140 ^oC for 6 h to dehydrate the system. After the toluene was removed at 150 ^oC for 4 h, this temperature was maintained for the polymerization. During the polymerization, the reaction mixture turned to a viscous brown solution. The viscous solution was obtained after 16 h of the reaction, and then it was cooled to room temperature and diluted with 10 mL of NMP. The polymer was obtained by precipitation in isopropyl

alcohol, followed by washing with DI water and isopropyl alcohol alternately for several times to completely remove the residual salts and solvent. The number average molecular weight (M_n) and polydispersity index (PDI) were 5,300 g/mol and 1.390, respectively.

^{1}H NMR (400 MHz, $CDCl_3$, TMS ref): δ = 1.66 (6 H, m, -CH_3 of DBPA), 3.23 (2 H, d, -*CH_2*--CH_2-*CH*=CH_2 of allyl groups), 6.93 (4 H, m, ArH ortho to -O-), 7.93 (4 H, d, ArH ortho to -SO_2-), 7.42 (2 H, s, ArH ortho to allyl groups), 6.38-7.94 (m, other ArH).

Preparation of allyl polysulfone-*graft*-poly(dimethylaminoethyl methacrylate) porous substrate (AMEA substrate).

AMEA porous substrate was prepared by *in situ* process composed of *grafting-through* polymerization followed by non-solvent induced phase separation (NIPS) method.[35,36] APSf (1.00 g), AIBN (0.09 g), PSf (1.00 g), and DMAMEA (0.8 g) were dissolved in 10.3 mL of NMP in a 100 mL dried Schlenk flask containing a magnetic stir bar. PSf is the commercial polysulfone and it was intentionally used to increase the stability of the membrane. The flask was sealed with a septum and deoxygenate with nitrogen for 1h. The flask was then placed in an oil bath maintained at 60 ^{o}C and stirred with a magnetic stir bar for 3 h for the

polymerization of vinylic monomer moieties in APSf and DMA, resulting in a clear yellow solution. After the polymerization, the resulting solution was left in sonication at degassing mode for 2 h to remove air bubbles trapped within the solution, followed by casting on a non-woven PET fabric using a doctor blade at a thickness of 100 μm, and then immersed into DI water bath at room temperature. A pristine PSf substrate was also prepared using the NIPS method for comparision, and the composition of PSf casting solution is listed in Table 1.

Preparation of thin film composite (TFC) membranes.

Interfacial polymerization with MPD and TMC was carried out to fabricate polyamide layer of TFC membrane. In the whole process, membranes were fixed in a rubber frame which only enabled the top layer of the substrates to participate in the interfacial polymerization. The AMEA and PSf substrate were immersed in a 2 wt% of MPD aqueous solution for 120 s. After removing the excess MPD solution by rolling a rubber roller, the top layer of the membrane substrate was brought into contact with a 0.1 wt% TMC solution in EA/*n*-hexane (1/50 v/v) for 30 s. After removing the TMC solution, the TFC membranes were dried in air for 240 s and then stored in DI water until testing. The as-prepared TFC membranes using the AMEA and PSf substrate were designated as TFC-AMEA and TFC-PSf,

respectively.

Characterization

Surface and cross-sectional morphologies of the membranes were investigated by scanning electron microscopy (SEM) using a field emission scanning electron microscope (FE-SEM, JEOL JSM-7800F) with an accelerating voltage of 10 kV. Before SEM measurements, samples were freeze-dried and coated with platinum using a JEOL JFC-1100E ion sputtering device. Surface chemical composition was studied using infrared (IR) spectra with an attenuated total reflectance (ATR) equipment (FT-IR/ATR, Nicolet 6700 spectrophotometer, Thermo Scientific). X-ray photoelectron spectroscopy (XPS) measurements were performed on an Axis-HIS XPS (PHI-1600, Kratos Analytical) applying Mg Ka (1254.0 eV) as a radiation source. XPS spectra were collected over a range of 0-1100 eV, followed by the high resolution scan of the C 1s, O 1s, and N 1s regions. Contact angle from air captive bubble in water were carried out a contact angle goniometer (Krüss DAS10) Contact angles for the substrates were measured for five times on three independently prepared substrates.

Reverse osmosis (RO) test

The water permeance (A, L^{-2} M^{-1} h^{-1} bar^{-1}, abbreviated as LMH/bar), salt rejection (R_s, %), and salt flux (B, LMH) were determined by using a lab-scale dead-end filtration system. All tests were carried out at 5 bar under room temperature with an effective membrane area of approximately 5.73 cm^2.

A value was calculated from pure water permeation fluxes under a trans-membrane pressure varying from 1 to 5 bar. The pure seater permeation flux was obtained by Equation(1):

$$J_v = \frac{\Delta V}{A \Delta t} \tag{1}$$

Where ΔV (L) is the volume of permeated solution collected between two weight measurements, A (m^2) is the membrane surface area, and Δt (h) is the time between two weight measurements.

R_s values were determined by carrying out the tests using a 2000 ppm of NaCl solution as the feed solution under a rapid stirring condition (700 rpm). R_s was calculated by Equation(2) as follows:

$$R_s = \left(1 - \frac{C_p}{C_s}\right) \times 100\ \% \tag{2}$$

Where C_p and C_s indicate the NaCl concentrations of permeate and feed solution, respectively.

B value was determined according to the solution-diffusion theory by using Equation (3).[17,21,22]

$$\frac{100 - R_s}{R_s} = \frac{B}{A\,(\Delta P - \Delta \pi)} \tag{3}$$

In Equation (3), ΔP (bar) is the applied pressure and re $\Delta \pi$ (bar) is the osmotic pressure difference across the membrane.

Forward osmosis (FO) test

FO experiments were conducted in a lab-scale cross-flow FO system, as depicted in Figure 1. The volume of the feed and the draw solutions was fixed as 2.0 L at the start of each experimental run. Two variable speed gear pumps were used to pump the feed and draw solution co-currently in closed loops with a crossflow velocity of 1 cm/s. The membrane cell had an effective channel dimensions of 2.0 cm long, 1.0 cm wide, and 3 mm deep for co-current crossflows. A water bath was used in order to maintain the temperature of the feed and draw solution at 25 ± 0.5 ^{o}C. All membranes were tested in AL-FS mode (the active layer was oriented towards the feed solution) and AL-DS mode (the active layer was oriented towards the draw solution). The weight change of the draw solution reservoir was simultaneously recorded to calculate the water permeation flux. Conductivity of

the feed solution was also measured by conductivity meter to estimate the reverse salt flux.

Fouling test

Fouling experiment was conducted in a lab-scale cross-flow FO system, as mentioned above. Before each experiment, the system was cleaned and disinfected by flushing sequentially with 10% bleach, 5 mM EDTA, and 95% ethanol for 1 h. Then, the system was rinsed for three times with DI water to remove the cleaning reagents.

An artificial secondary wastewater medium, with an ionic strength of 16 mM and pH of 7.6 ± 0.2, was used as a feed solution (see Table 2 for medium composition). 2 M NaCl solution was used as a draw solution and the active layer of membrane was oriented toward the draw solution (AL-DS mode). The weight change of the draw solution reservoir was simultaneously recorded to calculate the water permeation flux. Normalized flux variation was also obtained by diving the flux at certain time by the initial water flux.

3.3. Results and Discussion

Allyl polysulfone (APSf) was synthesized *via* the condensation polymerization of the dihydroxy monomer (2,2'-diallylbisphenol A (DBPA)) with the dihalo monomer (4,4'-difluorodiphenyl sulfone (DFDPS) where DBPA was intentionally used because the allyl group can go through the radical polymerization to introduce dimethylaminoethyl methacrylate (DMAEMA) by the *grafting-through* approach (Figure 2). A small amount of hydroquinone as a radical scavenger was added into the reaction mixture in order to prevent unintended isomerization of allyl groups in the DBPA.[13] Figure 3 shows ^{1}H NMR spectra and the assignment of the respective peaks of APSf. As expected, all of the corresponding resonance peaks of APSf were clearly found in the spectra. For example, the proton peaks from the allyl groups (δ = 3.23 and 4.95 ppm) indicate that the isomerization of the allyl group into the propenyl group was efficiently inhibited.[20]

A series of functional membranes consisted of allyl polysulfone-*graft*-poly(dimethylaminoethyl methacrylate) (AMEA substrate) was fabricated through the following three steps: (1) preparing dope solutions by the polymerization of vinylic monomer moieties in APSf and DMAEMA (grafting-through), (2) casting

the resulting solutions as films onto a PET non-woven fabric, and (3) immersing the films for 24 h in a DI water bath for the formation of membranes by non-solvent induced phase separation (NIPS) method (Figure 4). A clear and homogeneous solution containing allyl polysulfone-*graft*-poly(dimethylaminoethyl methacrylate) in which poly(dimethylaminoethyl methacrylate) (PDMAEMA) brushes are grafted onto the APSf macromonomer can be prepared from step (1)[42,43] Commercial polysulfone (PSf) was included in the reaction mixture to improve stability of the membranes, similar to our previous approach about the fabrication of ultrafiltration membranes. For the preparation of PSf substrate, more dilute casting solution was used than for the preparation of the AMEA substrate, because commercial polysulfone has larger molecular weight than APSf (50,000 g/mol and 5,300 g/mol for polysulfone and APSf, respectively). We could not handle the polysulfone solution above certain concentration to fabricate the membrane because it is too viscous.

Figure 5 illustrates ATR-IR spectra of the PSf and AMEA substrates exhibiting the characteristic peaks ascribable to PSf at 2968 cm^{-1}, 1584 cm^{-1}, and 1487 cm^{-1}, correspond to aromatic -C-H and -C-C stretching of polysulfone. Comparing the PSf with AMEA substrate, peak at -1727 cm-1 (O-C=O stretching) is newly observed in ATR-IR spectra of AMEA substrate, verifying the presence of PDMAEMA moieties.

Figure 6 and Table 3 show the pore size characteristics of the PSf and AMEA substrates. The average pore diameter of AMEA substrate is larger than that of PSf substrate, ascribed from the incorporation of hydrophilic PDMAEMA moiety in the AMEA substrate. The increase of hydrophilicity of the polymer casting solution can increase the exchange rate of solvent (NMP) with non-solvent (DI water) during the NIPS process, then larger pore can be obtained.[23-25]

The hydrophilicity of substrates was investigated by measuring air captive bubble contact angles on the membrane equilibrated in DI water (Table 3). The contact angle value of the AMEA substrate are smaller than that of the PSf substrate based on the presence of hydrophilic PDMAEMA moieties on the surface. It is remarkable to take note that the AMEA substrate has a larger pure water permeability (PWP) value than the PSf substrate, because the AMEA substrate has both larger average pore diameter than the PSf substrate. Additionally, it was found that hydrophilicitiy of the membrane increases water flux by stimulate the transport of water molecules during the pressurized filtration, the AMEA substrate could facilitate water molecules more rapidly than the PSf substrate.[26]

Polyamide selective layer was fabricated using the interfacial polymerization between *m*-phenylenediamine (MPD) and 1,3,5-benzenetricarbonyl trichloride (TMC) on the porous substrate, as shown in Figure 7. The resulting thin film

composite (TFC) membranes prepared from the PSf and AMEA substrates were designated as TFC-PSf and TFC-AMEA, respectively. The TFC-AMEA membrane was further treated by immersing the membrane into 1,3-propane sultone solution, to convert tertiary amine groups in PDMAEMA into zwitterionic groups through a straightforward alkylation process (TFC-SBMA).[27] Figure 8 presents the top surface morphology of the TFC-PSf, TFC-AMEA, and TFC-SBMA, indicating that all membranes exhibit a typical ridge-and-valley surfaces, while PSf and AMEA substrates show a dense and smooth surface.[28,29] Especially, there is no significant difference of polyamide morphology between TFC-AMEA and TFC-SBMA, supposing that the TFC-SBMA membrane can effectively reject contaminants in the feed stream. All TFC membranes have highly porous cross-sectional morphologies, composed of finger-like pore structures.

In order to confirm the presence of sulfobetaine moieties on the surface of TFC-SBMA membrane, XPS measurements were carried out using backside of the TFC-AMEA and TFC-SBMA membranes. In Figure 9, TFC-AMEA membrane shows single N 1s peak at 399.16 eV, attributable to the presence of PDMAEMA moieties in the membrane. After surface treatment, some neutral amino groups in PDMAEMA were transformed into quaternary ammonium cations, with showing newly assigned peak at around 401.06 eV. On the basis of XPS measurements, the

atomic composition of the membrane surface was calculated and demonstrated in Table 4, indicating that the atomic percentage of sulfur increases from TFC-AMEA to TFC-SBMA due to the successful zwitterionization on the membrane surface.

FO experiments were carried out by using a cross-flow filtration setup, using DI water as feed and various concentration of NaCl solutions as draw solutions. Figure 10 and Figure 11 show the experimental water permeation flux (J_v) and reverse solute flux (J_s) of TFC-PSf, TFC-AMEA, and TFC-SBMA membranes as a function of draw solution concentration. As shown in the figures, J_v values increase with increasing the concentration of draw solute for both testing modes. The fluxes level off at higher NaCl concentrations because of more severe ICP effect at higher draw solute concentration. It can be found that the water permeation flux values of the TFC-AMEA membrane are larger than those of TFC-PSf membrane, while their J_s values are of comparable values. TFC-SBMA membrane exhibits the largest J_v values at the same concentration, possibly due to the presence of more hydrophilic sulfobetaine moieties in the TFC-SBMA membrane compared to the TFC-AMEA membrane. The increase of J_v value with increasing the hydrophilicity of the substrate agrees with previous results,[30] confirming the enhancement of FO performance by using hydrophilic polymers as supports for TFC membranes.

Since reverse solute permeation has been reported as a critical FO performance parameter, J_s/J_v ratio is presented in Figure 12.[31,32] In all cases, this ratio gradually increases over a wide range of draw solute concentration in both testing modes. It was also found that the J_s/J_v ratio in AL-FS mode is smaller than that in AL-DS mode for all membranes, as similarly reported and discussed previously.[33] At the same concentration and testing mode, The J_s/J_v ratio of the TFC-AMEA membrane is smaller than that of the TFC-PSf membrane, while J_s/J_v ratio of the TFC-SBMA membrane is similar or smaller than that of the TFC-AMEA membrane. This result provides a significant possibility to purify water resources with minimizing the loss of draw solutes during the FO process when using the TFC-SBMA or TFC-AMEA membrane due to their hydrophilic substrate.

To determine the fouling mitigation potential of the membranes, dynamic fouling assays were conducted in a lab-scale cross-flow FO setup. An artificial secondary wastewater medium was used as a feed solution (Table 2).[34] In Figure 13(a), the largest initial water permeation flux value was observed when using the TFC-AMEA and TFC-SBMA membranes, due to their hydrophilic substrate. Over the course of 24 h, a gradual decline is observed in the water permeation flux due to the accumulation of fouling on the membrane surface. In case of TFC-PSf membrane, severe flux decline due to the fouling reaches 95% of

the initial flux after 24 h of operation, whereas flux decline for TFC-AMEA membrane was 60%, as shown in Figure 13(b). It is worth noting that the degree of flux decline is much less in the TFC-SBMA compared to the TFC-AMEA membrane, due to the presence of antifouling sulfobetaine moieties in the TFC-SBMA membrane.[35-38] This result indicates that reduced accumulation of membrane fouling is originated from both hydrophilicity and zwitterionic characteristics.

3.4. Conclusion

A hydrophilic substrate bearing tertiary amino moieties was successfully prepared by *grafting-through* approach and subsequent NIPS method without additional polymer pacification, in order to use the substrate as a support for the TFC membrane. Zwitterionization of the substrate was easily carried out by immersing the as-prepared TFC membrane after the interfacial polymerization, without any destruction of polyamide selective layer. Both TFC-AMEA and TFC-SBMA membranes show lower J_s/J_v ratios than the TFC-PSf membrane with reasonably high water fluxes. Especially, TFC-SBMA demonstrated a noticeable fouling resistance against synthetic wastewater, due to the zwitterionic moieties on the substrate. We strongly believe that newly developed TFC membranes could be

potentially used for industrial applications due to its facile preparation and excellent FO performances.

3.5. References

[1] Geise GM, Lee HS, Miller DJ, Freeman BD, McGrath JE, Paul DR. J Polym Sci Part B: Polym Phys 48 (2010) 1685-1718.

[2] Cath TY, Childress AE, Elimelech M. J. Membr Sci 281 (2006) 70-87.

[3] Chung T-S, Zhang S, Wang KY, Su J, Ling MM. Desalination 287 (2012) 78-81.

[4] McCutcheon JR, Elimelech M. AIChE J 53 (2007) 1736-1744.

[5] McGinnis RL, Elimelech M. Environ Sci Tehcnol 42 (2008) 8625-8629.

[6] Shannon MA, Bohn PW, Elimelech M, Georgiadis JG, Marinas BJ, Mayes AM Nature 452 (2008) 301-310.

[7] Zhao S, Zou L, Tang CY, Mulcahy D. J Membr Sci 396 (2012) 1-21.

[8] Chung T-S, Li X, Ong RC, Ge Q, Wang H, Han G. Curr Opin Chem Eng 1 (2012) 246-257.

[9] Elimelech M, Phillip WA. Science, 333 (2011) 712-717.

[10] Liu Z, Bai H, Lee J, Sun DD. Energy Environ Sci 4 (2011) 2582-2585.

[11] Emadzadeh D, Lau WJ, Ismail AF. Desalination, 330 (2013) 90-99.

[12] Gray GT, McCutcheon JR, Elimelech M. Desalination, 197 (2006) 1-8.

[13] McCutcheon JR, Elimelech M. J Membr Sci 284 (2006) 237-247.

[14] Wang KY, Ong RC, Chung T-S. Ind Eng Chem Res 49 (2010) 4824-4831.

[15] Zhang S, Wang KY, Chung T-S, Chen H, Jean YC, Amy G. J Membr Sci 360 (2010) 522-535.

[16] Widjojo N, Chung T-S, Weber M, Maletzko C, Warzelhan V. J Membr Sci 383 (2011) 214-223.

[17] Wang KY, Chung T-S, Amy G. AIChE J 58 (2012) 770-781.

[18] McCutcheon JR, Elimelech M. J Membr Sci 318 (2008) 458-466.

[19] Sahoo BB, Raj TT, Srinvasarao AR, Lens JP. Monomers for the preparation of silylated plycarbonate polymers, PCT Int. Appl., WO2008079358, 2008.

[20] Ni J, Zaho C, Zhang G, Zhang Y, Wang J, Ma W, Liu Z, Na H. Chem Commun 47 (2011) 8943-8945.

[21] Lee KJ, Baker RW, Lonsdale HK. J Membr Sci 8 (1981) 141-171.

[22] Loeb S, Mehta GD. J Membr Sci 4 (1978) 351-362.

[23] Lee J, Chae HR, Won YJ, Lee K, Lee CH, Lee HH, Kim IC, Lee JM. J Membr Sci 448 (2013) 223-230.

[24] Yu L, Zhang Y, Zhang B, Liu J, Zhang H, Song C. J Membr Sci 447 (2013) 452-462.

[25] Zhao H, Wu L, Zhou Z, Zhang L, Chen H. Phys Chem Chem Phys 15 (2013) 9084-9092.

[26] Chem Y, Ying L, Yu W, Kang ET, Neoh KG. Macromolecules 36 (2003) 9451-9457.

[27] Dundua A, Franzka S, Ulbricht M. Macromol Rapid Commun (2016) ASAP. doi: 10.1002/marc.201600473

[28] Ghosh AK, Jeong B-H, Huang X, Hoek EM. J Membr Sci 311 (2008) 34-45.

[29] Tiraferri A, Kang Y, Giannelis EP, Elimelech M. ACS Appl Mater Interfaces 4 (2012) 5044-5053.

[30] Widjojo N, Chung T-S, Weber M, Maletzko C, Warzelhan V. Chem Eng J 220 (2013) 15-23.

[31] Achilli A, Cath TY, Childress AE. J Membr Sci 364 (2010) 233-241.

[32] Xiao D, Tang CY, Zhang J, Lay WCL, Wang R, Fane AG. J Membr Sci 366 (2011) 314-324.

[33] Tiraferri A, Yip NY, Phillip WA, Schiffman JD, Elimelech M. J Membr Sci 367 (2011) 340-352.

[34] Perreault F. Jaramillo H, Xie M, Ude M, Nghiem LD, Elimelech M. Environ Sci Technol 50 (2016) 5840-5848.

[35] Baker JS, Dudley LY. Desalination 118 (1998) 81-90.

[36] Chang Y, Chang W-J, Shih Y-J, Wei T-C, Hsiue G-H. ACS Appl Mater Interfaces 3 (2011) 1228-1237.

[37] Chen W, Su Y, Peng J, Zhao X, Jiang Z, Dong Y, Zhang Y, Liang Y, Liu J. Environ Sci Tehcnol 45 (2011) 6545-6552.

[38] Xie M, Shon HK, Gray SR, Elimelech M. Water Res 89 (2016) 210-221.

Table 3.1. Preparation of the substrates

Sample	Macromonomer	Monomer	Initiator	Matrix	Solvent	Solid Concentration[a]
	APSf (g)	DMAEMA (g)	AIBN (g)	PSf (g)	NMP (mL)	(g/L)
PSf	0	0	0	2.0	14.4	0.14
AMEA	1.0	0.8	0.09	1.0	10.3	0.30

[a] Solid concentration was obtained by dividing the sum of moles of solid content (APSf, DMAEMAIBN, and PSf) by the volume of NMP.

Table 3.2. Composition of synthetic wastewater.

Reagent	Concentration (mM)
Glucose	0.6
NH_4Cl	0.4
$KHPO_4$	0.2
$CaCl_2$	0.1
$NaHCO_3$	0.5
NaCl	8
$MgSO_4$	0.15

Table 3.3. Intrinsic properties of the membranes.

Sample	Average pore diameter (nm)	Contact angle (^{o})	Pure water permeability (LMH)
PSf	10.0	80.6 ± 1.9	683.6 ± 42.2
AMEA	14.7	50.9 ± 0.9	817.6 ± 25.4

Table 3.4. XPS elemental composition (in at%) of the backside of TFC-AMEA and TFC-SBMA membranes.

	Elemental composition (in at%)				N/S ratio
	C 1s	O 1s	N 1s	S 2p	
TFC-AMEA	77.46	18.94	2.61	0.99	2.64
TFC-SBMA	81.40	19.31	1.84	1.30	1.42

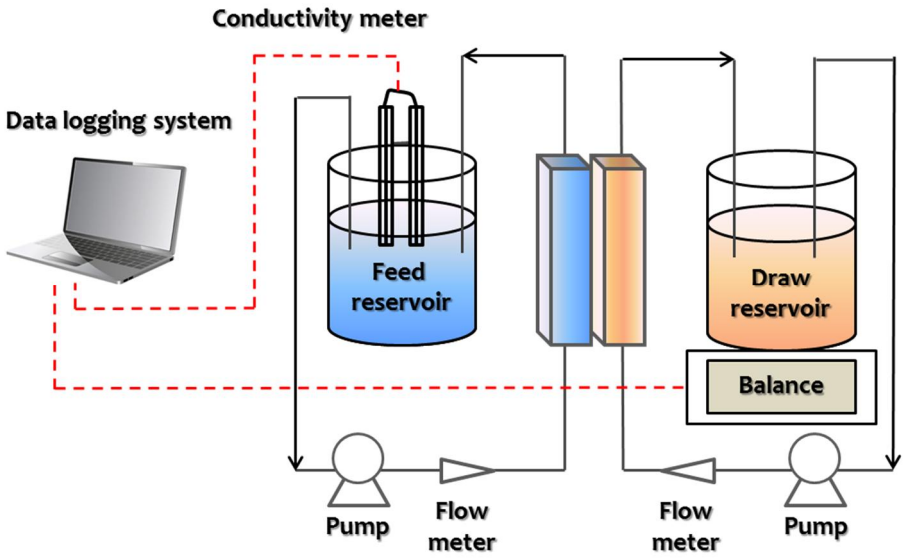

Figure 3.1. Forward osmosis (FO) experimental setup for testing the membranes.

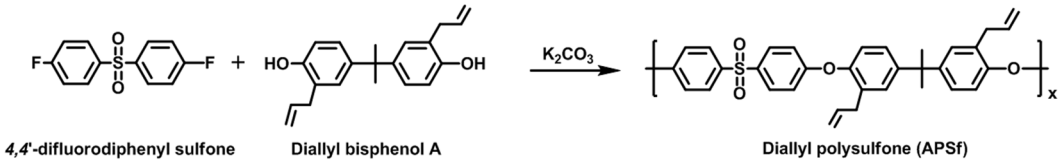

Figure 3.2. Synthesis of allyl polysulfone (APSf).

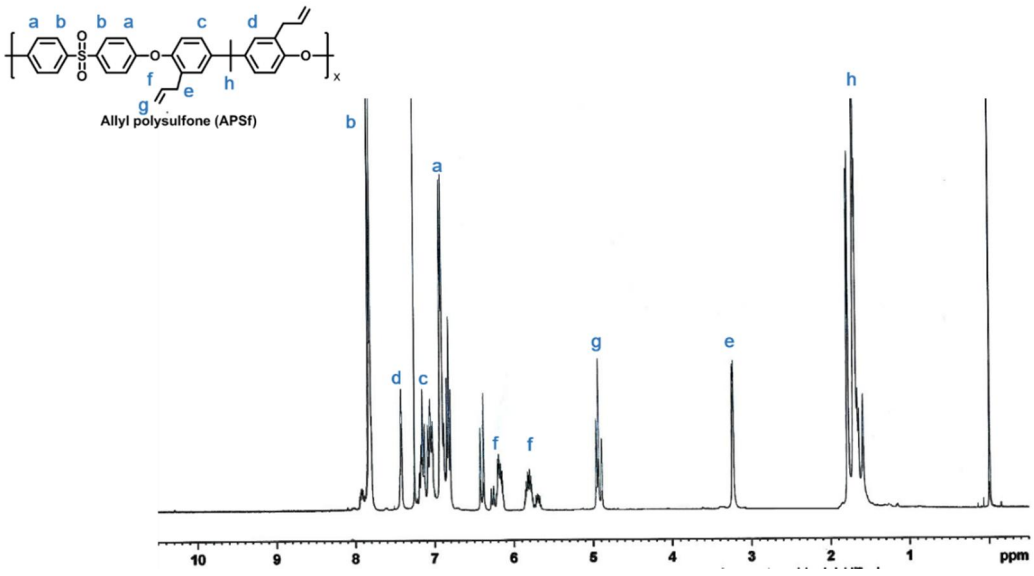

Figure 3.3. ^{1}H NMR spectra of allyl polysulfone (APSf) synthesized in the presence of hydroquinone (HQ).

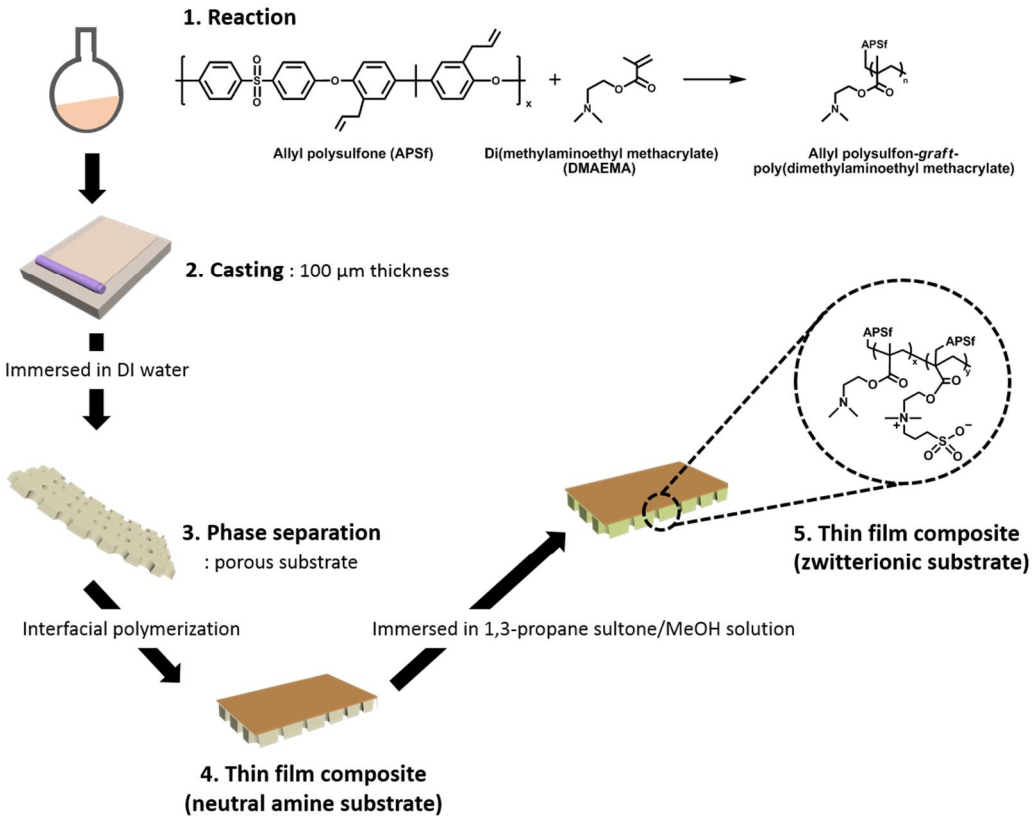

Figure 3.4. Preparation of the functionalized substrate using the as-prepared dope solution containing allyl polysuflone-*graft*-poly(dimethylaminoethyl methacrylate) (AMEA substrate).

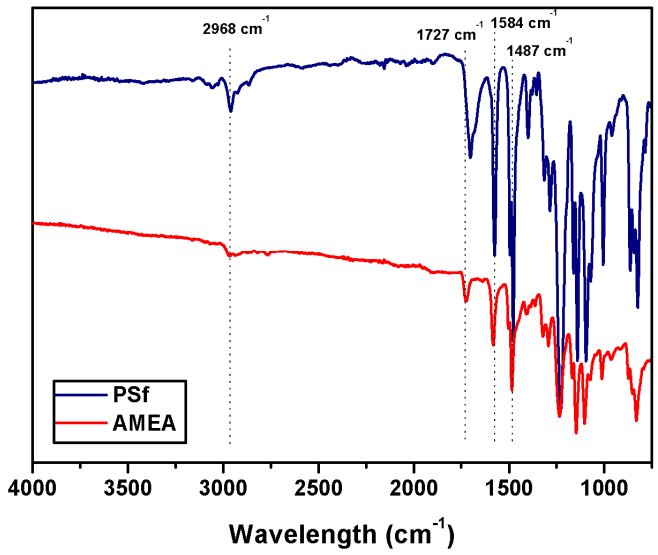

Figure 3.5. ATR-FTIR spectra of polysulfone (PSf) and the AMEA substrate.

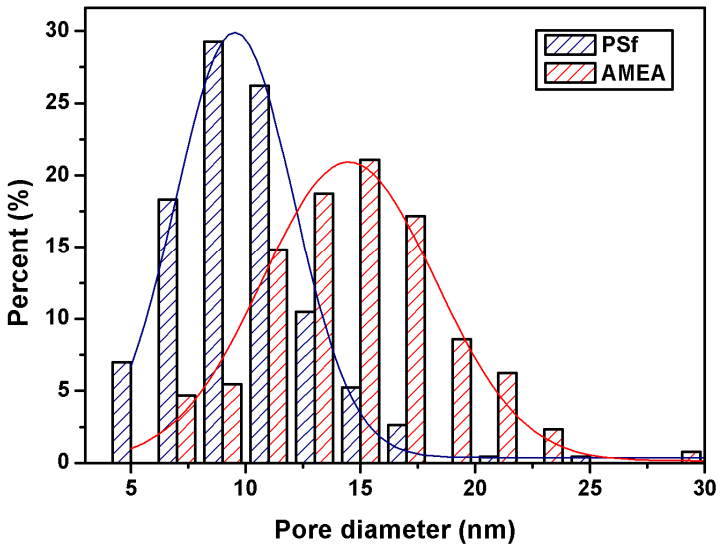

Figure 3.6. Pore size distribution of PSf and AMEA substrates.

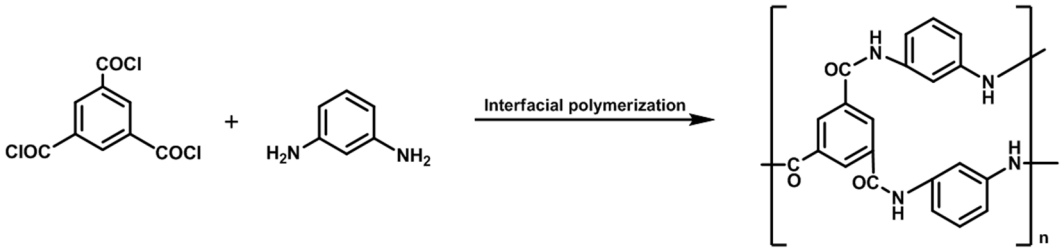

Figure 3.7. Reaction between m-phenylene diamine (MPD) and 1,3,5-tricarbonyl trichloride (TMC).

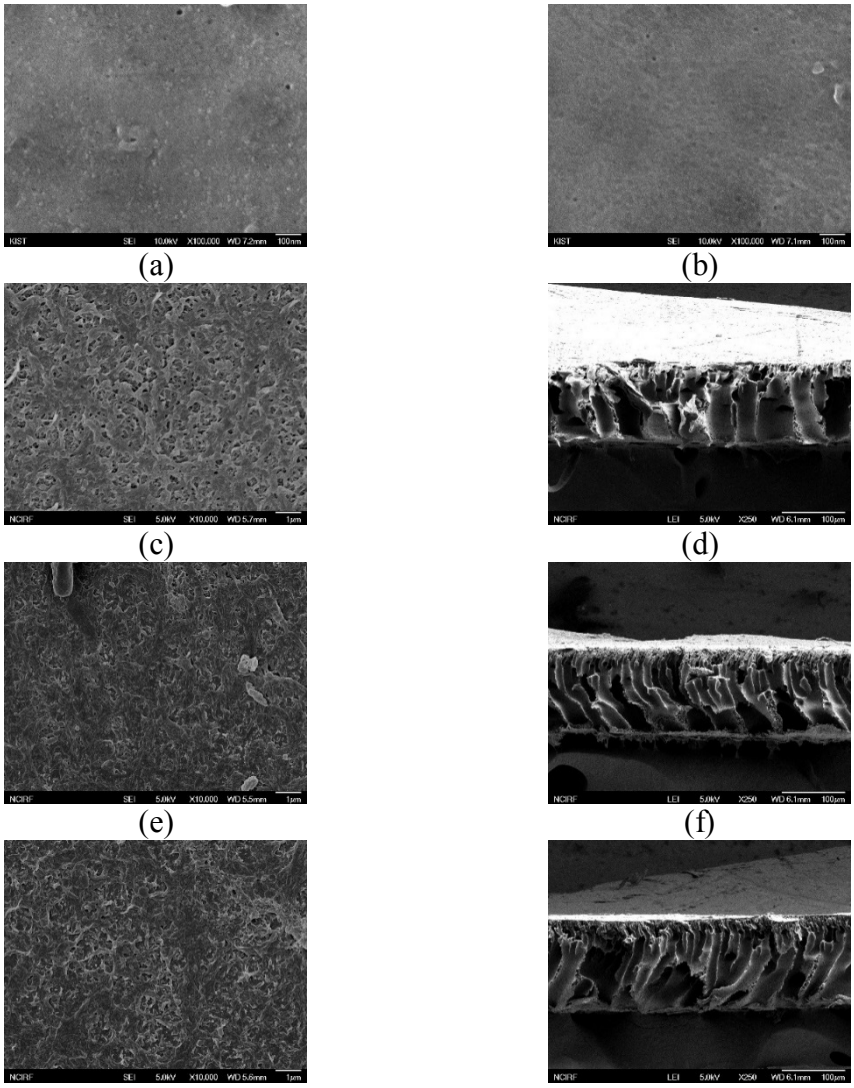

Figure 3.8. FE-SEM micrographs of (a) PSf, (b) AMEA, (c,d) TFC-PSf, (e,f) TFC-AMEA, and (g,h) TFC-SBMA membranes.

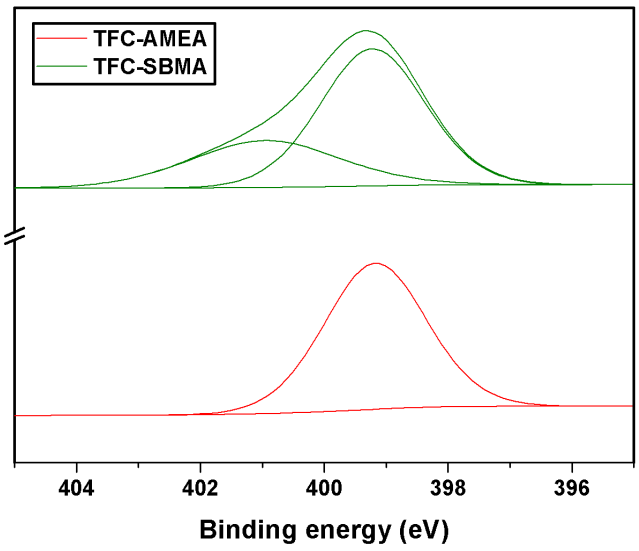

Figure 3.9. XPS N 1s core level spectra of the backside of TFC-AMEA and TFC-SBMA membranes.

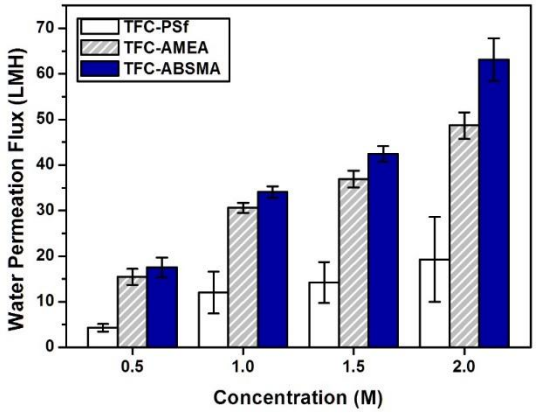

(a)

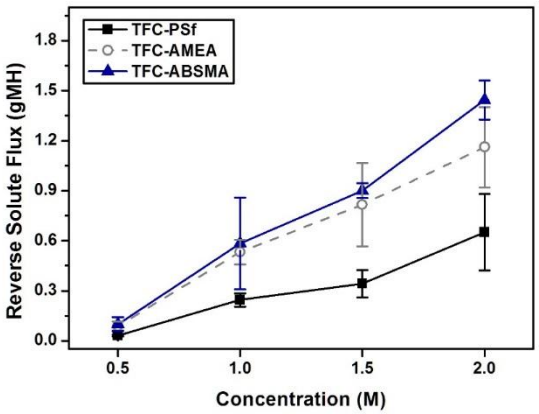

(b)

Figure 3.10. (a) Water permeation fluxes (J_v) and (b) reverse solute fluxes (J_s) of TFC membranes under AL-DS mode using different draw solute concentration.

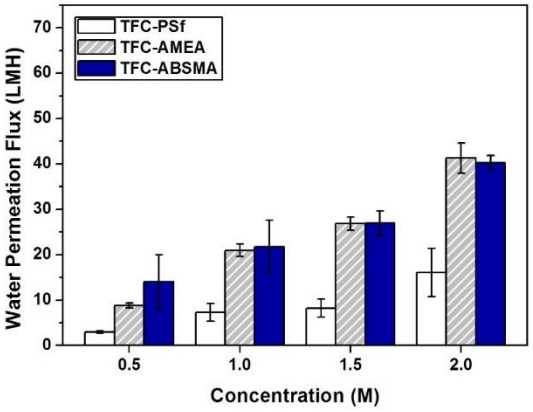

(a)

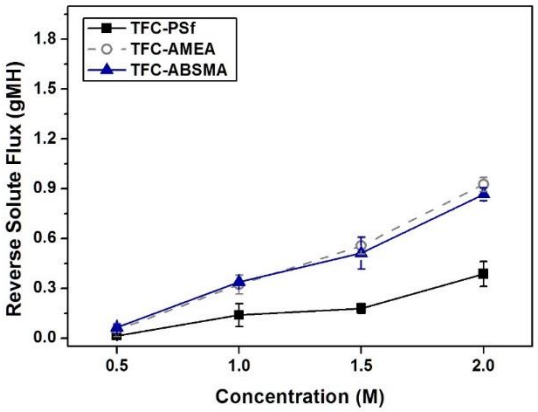

(b)

Figure 3.11. (a) J_v and (b) J_s values of TFC membranes under AL-FS mode using different draw solute concentration.

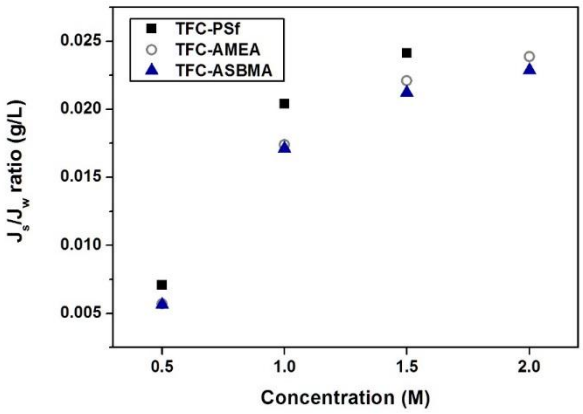

(a)

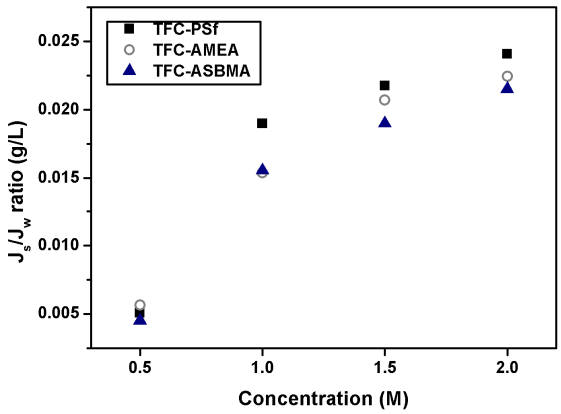

(b)

Figure 3.12. J_s/J_v ratios in (a) AL-DS mode and (b) AL-FS mode.

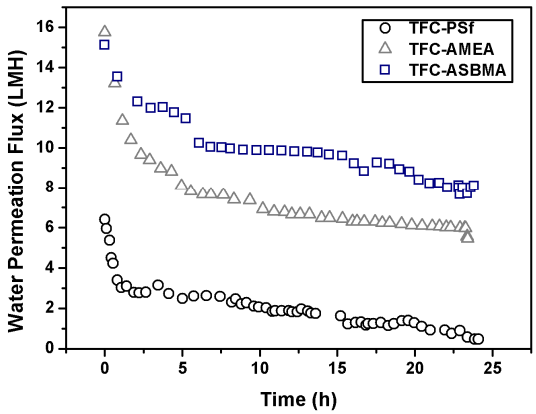

(a)

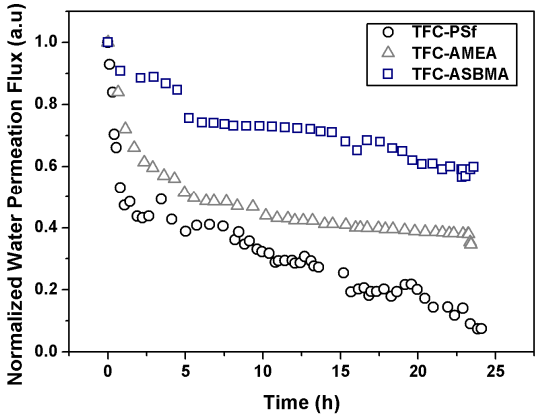

(b)

Figure 3.13. Time dependence of water permeation flux variations during the filtration of synthetic wastewater: (a) flux behavior and (b) normalized flux behavior.

Chapter 4

Oligomeric Draw Solutes for FO Application

4.1. Introduction

Water scarcity has emerged recently as a global problem due to the increasing demand for fresh water as a result of the increasing global population, water pollution, and climate change [1,2]. A number of studies have focused on water treatment technologies to alleviate the water shortage problem and also to improve the quality of treated [3–6]. Among the water treatment technologies, the forward osmosis (FO) system has drawn much attention due to the advantages in energy consumption. In the FO system, the high osmotic pressure between the feed and draw solutions is used to induce the diffusion of water molecule through a semi-permeable membrane from the feed to the draw solution [7]. Therefore, the FO system has been studied intensively in various applications such as desalination [8], wastewater treatment [9], food processing [10], protein concentration [11,12], energy production [13], and so on [1]. However, the practical application of the FO system has been limited because of the remaining obstacles such as the absence of both adequate draw solute systems and efficient membranes [14].

Many studies have focused on the exploration of proper draw solutes that demonstrate several characteristics such as high water solubility, high osmotic pressure, high water permeation flux, low reverse solute flux, and efficient

recovery [15]. For example, sugars [16,17], organic and inorganic salts [18,19], hydrogels [20,21], polyelectrolytes [22-25], magnetic nanoparticles [26–28], metal-acid complexes [29,30], and carbon quantum dots [31] were studied as draw solutes, while the task of the development of draw solute systems that have both high FO performances and recovery efficiency still needs to be carried out [2,14].

Recently, thermal treatment for recovery in the FO system has received growing attentions as an effective recovery method for draw solutes because the waste heat and/or geothermal heat can be used as the heat source [32]. If polymers having lower critical solution temperature (LCST) are used as the draw solute, the polymers in the draw solution could be separated easily by heating them to above their LCST followed by a membrane filtration process [33–37]. These polymers could be prepared by the copolymerization of thermo-responsive monomers, such as *N*-isopropylacrylamide and di(ethylene glycol)methyl methacrylate, with ionic monomers such as sodium styrene-4-sulfonate, sodium acrylate, and [2-(methacryloyloxy)ethyl]-trimethylammonium chloride. The draw solutions of the resulting polymers obtained with the copolymerization showed reasonable water permeation flux and the purified water and the polymers could be separated using the membrane filtration method as reported by the authors and by others [24,32,33,37]. Still the FO water permeation flux values of these systems are not

high enough for practical application because of the presence of nonionic thermo-responsive moieties and high molecular weights of the copolymers [24,33].

As a continuous effort to develop the thermo-responsive polymers for the draw solute, thermo-responsive oligomeric poly(tetrabutylphosphonium styrenesulfonate) (PSSP#) was prepared in this study because other poly(styrenesulfonate) derivatives were known to have the LCST in a very narrow range as reported by Kohno et al [38–40]. The effect of molecular weight of the PSSP on the osmotic pressure, water permeation flux, reverse solute flux, and LCST behavior was systematically observed here. Recovery of the draw solute from the solution could be simply achieved by mild heating at 60 ^{o}C followed by separating the supernatant liquid from the precipitated polymer without any membrane process. In addition, the PSSP solutions showed a bactericidal property, and the possible biofilm formation that decreases the membrane performance [41] then could be minimized.

4.2. Experimental

Materials

Tetrabutylphosphonium bromide (98 %), deionized water (for TOC analysis), and methyl orange (85 %) were purchased from Sigma-Aldrich Co., LLC. and used as received without further purification. Sodium p-styrenesulfonate hydrate (93 %) was purchased from Tokyo Chemical Industry Co., LTD. and used without further purification. 2,2'-Azobis(isobutyronitrile) (AIBN) was purchased from Junsei Chemical Co., Ltd. and purified by recrystallization from ethanol. n-Hexane (95%), diethyl ether, and sodium chloride (NaCl, 99.5 %) were purchased from Daejung Chemicals & Metals Co., LTD. and used as received. Ethanol was purchased from Hayman Chemical Co. and dried over a molecular sieve (4 Å). The dialysis membrane was purchased from Membrane Filtration Products, Inc. having 1,000 Dalton of the nominal molecular weight cut off (MWCO). *Escherichia coli* (*E. coli*; ATCC 8739) were obtained from the American Type Culture Collection (ATCC). BactoTM Agar and DifcoTM Nutrient Broth were obtained from Becton, Dickinson and Company (BD). Other reagents were used as received.

Synthesis of tetrabutylphosphonium styrenesulfonate (SSP)

Tetrabutylphosphonium styrenesulfonate (SSP) was synthesized according to the reported procedures, as shown in Figure 4.1 [39]. Sodium p-sytrenesulfonate hydrate (1.68 g, 8 mmol) and tetrabutylphosphonium bromide (4.00 g, 12 mmol) were dissolved in deionized water (10 mL) in a 100 mL round bottom flask containing a magnetic stir bar. After stirring at room temperature for 1 h, the product was extracted with dichloromethane three times, followed by drying over anhydrous magnesium sulfate. The solution was then concentrated using a rotary evaporator to obtain an oily liquid product.

^{1}H NMR of SSP [400 MHz, D2O, δ/ppm]: 0.92 (t, 12H, P-(CH_2-CH_2-CH_2-*CH_3*)$_4$), 1.35-1.41 (m, 16 H, P-(CH_2-*CH_2*-*CH_2*-CH_3)$_4$), 2.00-2.08 (m, 8 H, P-(*CH_2*-CH_2-CH_2-CH_3)4), 5.45 (d, 1 H, *CH_2*=CH-Ph), 5.93 (d, 1 H, *CH_2*=CH-Ph), 6.83 (t, 1 H, CH_2=*CH*-Ph), 7.62 (d, 2 H, CH_2=CH-*Ph*), and 7.78 (d, 2 H, CH_2=CH-*Ph*).

Synthesis of oligomeric poly(tetrabutylphosphonium styrenesulfonate) (PSSP#)

A series of oligomeric poly(tetrabutylphosphonium sytrenesulfonate) (PSSP#, where # is the number of repeat units) was synthesized by varying the amount of

initiator, AIBN as follows. SSP (3.0 g, 6.78 mmol) and AIBN (0.011 g, 0.07 mmol) were dissolved in ethanol (11.41 mL) in a 100 mL dried Schlenk flask containing a magnetic stir bar. The flask was sealed with a septum and deoxygenated with nitrogen for 1 h. The flask was then placed in an oil bath controlled at 60 ^{o}C and stirred with a magnetic bar for 3 h. After removing the solvent by vacuum evaporation, the polymer was dissolved in 5 mL of chloroform and precipitated in n-hexane three times. The resulting polymer was dialyzed against deionized water using dialysis membranes (MWCO = 1,000 Dalton) for 3 days. After evaporating the deionized water, the product was dried under vacuum at room temperature. The molecular weight of this product was measured using a matrix-assisted laser desorption ionization-time of flight (MALDI-TOF) mass spectrometry found to be about 4,700 Dalton, and it corresponds to the number of repeating units of 10.69. To distinguish this product with other PSSP having different molecular weights, it was named PSSP11, where '11' indicates the approximate number of the monomeric unit in the oligomer. Other oligomeric PSSPs were also prepared using the same procedure except for the amount of the initiator. For example, when 0.055 g (0.34 mmol) and 0.22 g (1.36 mmol) of AIBN was used, the molecular weights of the resulting product measured using MALDI-TOF mass spectrometry were found to be 2,600 and 2,100 Dalton, respectively, and they were named PSSP6 and PSSP5 because their molecular weight corresponds to

5.84 and 4.84 monomeric units, respectively.

^{1}H NMR of PSSP11 [400 MHz, D_2O, δ/ppm]: 0.82 (t, 12 H, P-(CH_2-CH_2-CH_2-*CH_3*)$_4$), 1.35-1.41 (m, 16 H, P-(CH_2-*CH_2*-*CH_2*-CH_3)$_4$), 2.00-2.08 (m, 8 H, P-(*CH_2*-CH_2-CH_2-CH_3)$_4$), 6.18-6.90 (s, 2 H, CH_2-CH-*Ph*-SO_3), 7.30-7.88 (s, 2 H, CH_2-CH-*Ph*-SO_3).

Characterization

The molecular weights were obtained using MALDI-TOF mass spectrometry (AB SCIEX TOF/TOFTM 5800 System, Applied Biosystems, USA) with a linear detector. The osmolality values of the PSSP series were obtained by measuring the freezing point depression using a semi-micro osmometer (K-7400, KNAUER, Germany). The osmolality values were adequately changed to the osmotic pressure by van't Hoff equation using the temperature and density of the solution (T = 297 K, density = 1 g/ml), then 1 Osmol/kg could be converted to the osmotic pressure of 24.354 atm. The dynamic viscosities of the SSP and PSSP solutions were measured using a stress controlled rheometer (Discovery Hybrid Rheometer, DHR-3, TA Instruments, USA) using parallel plate geometry (22 mm diameter). Lower critical solution temperature (LCST) values of the SSP and the PSSP solutions were measured by observing the optical transmittance at a wavelength of

650 nm using UV-Vis spectrophotometer (Agilent 8453E, Agilent Technologies Inc., USA) by increasing the temperature from 30 to 70 ^{o}C at a heating rate of 1 oCmin-1. The water content in the PSSP gel was measured using Karl-Fischer titrator (870 KF Titrino plus, Metrohm, USA). The total organic carbon (TOC) values were measured from the TOC Analyzer (Sievers 5310C, General Electric Co., LTD., USA). The polymer content of the thermally recovered solution was analyzed using ion chromatography (DX-120, Thermo Fischer Scientific, Inc., USA) with conductivity detection.

Forward osmosis (FO) test

The water permeation flux was measured using a small-scale custom forward osmosis (FO) system by connecting two L-shaped glass tubes settled with plastic caps [33]. A thin film composite FO membrane from Hydration Technologies Inc. (HTI) was placed in a circular channel (1.0 cm in diameter) between the two glass tubes. One tube was filled with deionized water or a NaCl solution as the feed solution, while the other contained the PSSP solution as the draw solution. During the FO tests, the temperatures of the feed and draw solutions were maintained at 25 ± 1 °C and stirred with magnetic stir bar. The water permeation flux, J_v ($Lm^{-2}h^{-1}$, abbreviated as LMH), was calculated from the volume change of the draw

solution using equation (4.1):

$$J_v = \frac{\Delta V}{A\Delta t} \tag{4.1}$$

where ΔV (L) is the volume change of the draw solution over a time Δt (h), and A is the effective surface area (m^2) of the membrane calculated as 7.854×10^{-5} m^2. The reverse solute flux (J_s) was determined by analyzing the amount of draw solute diffusing into the feed solution and calculated by measuring the TOC value of the feed solution.

Separation of water and PSSP from the draw solution

Thermal precipitation was employed to separate the water from the draw solutions using 5 mL of 20 wt% aqueous solutions of SSP and PSSPs because the FO performances using these solutes were tested at 20 wt%. As a separate experiment, a small amount (0.1 mL) of the methyl orange dye was added to the PSSP aqueous solution to clearly observe the separation of the PSSPs from the solutions because the SSP and the PSSPs gels, obtained at above their LCSTs, are transparent and, therefore they cannot be easily distinguished from the transparent water with the naked eye, especially from the picture. After the solutions were heated to 60 ^{o}C for 1 h, the supernatant liquid at the top part of the draw solution

could be simply separated by pouring or by using suction process with syringes. The remaining amount of SSP or PSSP in the supernatant liquid was analyzed using ion chromatography. The water purification efficiency could be estimated by calculating the draw solute recovery rate (R) using equation (4.2):

$$R\,(\%) = \frac{C_{\mathrm{b}}\text{-}C_{\mathrm{a}}}{C_b} \times 100 \qquad (4.2)$$

where C_b and C_a (mg/L) are the content of the SSP or the PSSP before and after the separation processes, respectively.

Bacterial test

The antibacterial activity of PSSPs was tested against *Escherichia coli* (*E. coli*; ATCC 8739). To prepare the bacteria suspension, E. coli was cultured in the corresponding broth solutions at 37 ^{o}C foerr 18 h. A single colony was lifted off with a platinum loop and cultured in a shaking incubator for 18 h at 37 ^{o}C on a nutrient broth. After washing twice with phosphate buffered saline (PBS) to remove the culture medium, the bacterial suspension was diluted to give an initial concentration of a 1×10^6 colony forming unit (CFU) per mL [42]. The concentration of the bacterial cell was calculated by measuring the absorbance of the cell dispersions at 600 nm and referenced to a standard calibration curve. An

optical density of 0.1 at 600 nm is approximately equivalent to 108 cells per mL [43]. Each 15 mg of the PSSP sample was diluted in 4.5 mL of a PBS buffer, followed by mixing with 0.5 mL of the bacterial suspension containing 10^6 CFU/mL. The mixed solution was incubated at 37 ^oC with gentle agitation in a shaking incubator. After 24 h of incubation, the resulting solution was serially diluted and then 0.1 mL of each diluent was spread onto the agar plates. Viable microbial colonies were counted after being incubated for 18 h at 37 ^oC. Each test repeated at least three times. The bactericidal property was calculated as follows:

$$\text{Bactericidal property (\%)} = \frac{N_0 - N_i}{N_0} \times 100 \qquad (3)$$

where N_0 is the bacterial CFU of the blank sample and N_i is the bacterial CFU of the tested sample [43].

4.3. Results and Discussion

A series of oligomeric poly(tetrabutylphosphonium styrenesulfonate) (PSSP) was synthesized via free radical polymerization (FRP) using 6.78 mmol of SSP and different amount of a radical initiator, AIBN (Figure 4.1 and Table 4.1). PSSPs prepared using 20, 5, and 1 mol% of the initiator to the amount of the monomer, SSP, show the peak maximum values at 2100, 2600, and 4700 Dalton from the MALDI-TOF mass spectrometry and were designated as PSSP5, PSSP6, and PSSP11 because their calculated numbers of monomeric repeating units are 4.84, 5.84, and 10.69 respectively (Figure 4.2). Their molecular weights could not be obtained using aqueous gel permeation chromatography (GPC), which is known as a suitable technique for analyzing the molecular weight of polymers, because the polyelectrolyte having ionic characteristics can be easily adsorbed to the surface of a stationary phase in the GPC column [44,45]. Although the peak maximum values from the MALDI-TOF mass spectrometry might not exactly indicate the molecular weight of the polymers, such as number average and weight average molecular weight, the peak maximum values are still known to represent the approximate molecular weight of the oligomers and polymers as reported by others [46,47]. Since the peak maximum values such as 2100, 2600, and 4700 representing 4.84, 5.84, and 10.69 monomeric units, respectively, were

observed, PSSP5, PSSP6, and PSSP11 were used as the abbreviations for the samples. It was clearly shown that the decrease in the amount of initiator from 20 mol% to 1 mol% compared to the amount of the monomer increases the molecular weight, as expected. The chemical structures of the PSSPs were confirmed by ^{1}H NMR as shown in Figure 4.3, where PSSP11 is shown as a representative; signals at 5.44 and 5.93 ppm from the methylene protons of the double bond in the monomer (styrenesulfonate) disappear after the polymerization, while the other peaks from the methylene protons of the alkyl chain in tetrabutylphosphonium and the hydrogens attached to the aromatic rings in the styrene repeat unit remains.

Figure 4.4 shows the viscosity behavior of the SSP and PSSP solutions at different concentration. The viscosity of the draw solution substantially affects the efficiency of FO process. If the viscosity of the draw solution is too high, the diffusion of the draw solute in the draw solution will be significantly restricted, resulting in the large decrease of osmotic potential between the feed solution and draw solutions [48]. As shown in Figure 4.4, it was found that the viscosity value rapidly increases with the increase of the concentration as expected from the other draw solute systems by other [23,49]. The viscosity values of PSSP5 and PSSP6 are relatively small compared to those of PSSP11 because they have smaller oligomeric number of repeat units. Although PSSP11 shows larger viscosity

values than SSP, PSSP5, and PSSP6, subsequent experiments indicate that PSSP11 also have considerably high water permeation flux.

Osmotic pressure was examined using the freezing point depression method in order to investigate the possible application of the PSSPs as a draw solute because the osmotic difference between the feed and draw solutions is the driving force of the FO system. The osmotic pressure of the SSP and PSSP solutions is described in Figure 4.5 and Table 4.2 as a function of the concentration (weight percent, wt%) of the samples in water. It was observed that the osmotic pressure increases with increasing the concentration as expected by the other's results of the monoelectrolytes and polyelectrolytes obtained [18]. Additionally, the osmotic pressure decreases from SSP to PSSP11 for all of the concentration ranges, because of the well-known colligative property commonly observed from the polyelectrolytes [23,50]. Although they have same weight concentration, molality of SSP is higher than that of PSSP because the molecular weight value of PSSP is larger than that of SSP, resulting in the higher osmotic pressure of SSP than those of PSSPs. However, the decrease of the osmotic pressure values from SSP to PSSP11 was found to be not very much significant. Such small osmotic pressure change of the polyelectrolyte with the change of the molecular weight was predicted before by others [51,52]. It was reported that osmotic pressure is more affected by the concentration of the free counter ion; in our case

tetrabutylphosphonium ion is the free counter ion. Since SSP and PSSPs have the same monomeric structure, when they have same weight concentration, they should have the same tetrabutylphosphonium ion concentration. Therefore, the osmotic pressure of SSP and PSSPs were found to be not much different.

The application of the PSSPs as the draw solute in the FO system was evaluated by measuring the water permeation flux and reverse solute flux values in the AL-DS mode (the draw solution facing the active layer) as shown in Figure 4.6 and Table 4.2. The water permeation flux increases with the increase of the concentration of draw solution as expected from the changes of the osmotic pressure behavior, as shown in Figure 4.6(b) and Figure 4.7. Although the average pore size of the FO membrane is small enough to reject the SSP and PSSP molecules, the reverse solute flux value was observed because the membrane is not a perfect barrier as reported in the previous studies [53,54]. The reverse solute flux (RSF) was found to increase with increasing the concentration of draw solution, because the concentration gradient across the active layer, which determines the RSF, also increases with the concentration [55]. For example, the water permeation flux value of PSSP5 increases from 7.58 to 14.50 LMH when the concentration increases from 10 to 20 wt%, while the RSF value also increases from 0.11 to 0.14 gMH. The ratio of water permeation flux (J_v) and RSF (J_s) was calculated and demonstrated in Figure 4.8, indicating that J_s/J_v ratio shows no

obvious relationship with the concentration, while the J_s/J_v ratio certainly decreases with increasing the molecular weight of PSSP. Especially, the J_s/J_v ratio exhibits a significant decrease from SSP to PSSP5, implying that the PSSP requires much less operating cost for the operation compared to the SSP or other ionic salts [18].

Figure 4.9 illustrates the water permeation flux, the RSF, and the viscosity values as a function of the number of repeat units at 10 wt% concentration. As expected from the osmotic pressure behavior, the increase of the molecular weight (or the number of repeat units) of the draw solute decreases the RSF as well as the water permeation flux. For example, the water permeation flux values of SSP, PSSP5, PSSP6, and PSSP11 at 10 wt% concentration are 8.02, 7.58, 7.43, and 6.32 LMH, respectively, indicating that the decrease of the water permeation flux by increasing the molecular weight 11 times from SSP to PSSP11 is not significant about 21.2 % decrease. However, the changes of the RSF values were found to be significant; those for SSP, PSSP5, PSSP6, and PSSP11 at 10 wt% concentration are 0.29, 0.11, 0.05, and 0.01 gMH, respectively, indicating that the RSF value deceases by 96.6 % from SSP to PSSP11. At 20 wt% concentration, the decrease of water permeation flux values from SSP to PSSP11 is about 19.3 %, while the decrease of RSF values is 64.9 %. Such large decease of the RSF values could be attributed from the Gibbs-Donnan effect that large anionic backbones of

the PSSPs restrict the back-diffusion of their free counter ions through a semi-permeable membrane [55]. Likewise, it is well-known that the RSF decreases along with the increase in the molecular size of the draw solute [56], which can be estimated by measuring the viscosity of the draw solution [57]. We also found that PSSP having larger viscosity value such as PSSP11 has smaller RSF value than SSP. However, the larger decrease of RSF from SSP to PSSP5 could not be explained by the viscosity because only small increase of the viscosity are observed.

The lower critical solution temperature (LCST) was observed by measuring the optical transmittances using an UV-Vis spectrophotometer at 650 nm. A reversible phase change of PSSP obtained by heating and cooling the PSSP11 aqueous solution is representatively shown in Figure 4.10. Below the LCST, SSP and PSSP are soluble in water, but it becomes insoluble upon heating [39,58]. They can show the LCST behavior because of the changes of the interactive forces between water with polystyrenesulfonate anions or tetrabutylphosphonium cations and those between polystyrenesulfonate anions with tetrabutylphosphonium cations [59]. The PSSP solution becomes homogeneous when the temperature was lowered below its LCST because the interactive force between water with the PSSP becomes larger than that between polystyrenesulfonate anion and tetrabutylphosphonium cation again. Therefore, PSSP is soluble in water during

the membrane process, while it becomes insoluble in the draw solute recovery process. Similarly, LCST behavior was observed from nonionic polymers due to the changes of the hydrogen bonding force between the water with the polymeric moieties as well as that between the polymeric moieties themselves [60]. Figure 4.11 shows the transmittance change of the SSP and the PSSPs as a function of temperature at 10 wt% and 20 wt% concentrations, respectively; LCSTs, the temperatures when the transmittance drops abruptly, of PSSPs are higher than those of SSP. The higher LCST of the polymer than the monomer having the same unit structure was reported from others [39,61]. According to the previous reports, the SSP forms many small aggregates composed of styrenesulfonate anions and tetrabutylphosphonium cations, while the PSSP forms big aggregates composed of polystyrenesulfonate anions and tetrabutylphosphonium cations. Since the formation of a big aggregate requires higher energy to overcome the steric hindrance than that of a small aggregate, LCST of the PSSPs is higher than that of the SSP. In addition, polymer chain structure can more effectively shield any hydrophobic units in the molecule than the monomer structure [60,62].

Meanwhile among the PSSPs, LCST was found to decrease slightly with the increase of the molecular weight. For example, the LCST of PSSP11 at 20 wt% was 45 ^{o}C, while that of PSSP6 and PSSP5 were 46 and 47 ^{o}C, respectively. This result can be explained by the thermodynamic theory of the polymer solutions

(polymers mixed with low molecular weight solvents) having the LCST conditions where the Flory-Huggins interaction parameter (χ_c) was used to predict the LCST.[63]

$$\chi_c = \frac{1}{2}\left(1 + r^{-\frac{1}{2}}\right)^2 \tag{4.4}$$

where, r is the ratio of molar volumes of polymer and solvent. When the free volume dissimilarity between polymer and solvent increases, then χ_c increases. The increment of χ_c implies the decrease of the solubility of polymers in solvents. Therefore, the increase of the molecular weight of the polymers in the solutions decreases the LCST. The combination of the shielding effect and χ_c should result in the increase in the LCST from SSP to PSSP series and the small decrease of the LCST from PSSP5 to PSSP11. It was also observed that the LCST decreases with the increase of the concentration as shown in Figure 4.12 because the hydrated gels can be more easily formed for the electrolytes with high concentration [62]. For example, the LCST of PSSP5, PSSP6, and PSSP11 decreased from 54, 52, and 49 ^{o}C to 47, 46, and 45 ^{o}C, respectively, when the concentration was increased from 10 to 20 wt%.

The simplicity for the separation of the PSSPs from the water is representatively shown in Figure 4.13, whereby 20 wt% of PSSP11 aqueous solution was heated to 60 ^{o}C for 1 h. Although PSSP gels are formed above their

LCSTs, they could not be easily distinguished from the transparent water by the naked eye and pictures. Therefore, we intentionally added a small amount of methyl orange to easily distinguish between the gel and the water. The top water layer separated from the PSSP gels could be easily collected simply by pouring or using a syringe. The concentrations of the PSSPs in the supernatants were analyzed using ion chromatography to determine the draw solute recovery (R) values. The R values for the SSP, PSSP5, PSSP6, and PSSP11 solutions were found to be 99.33, 99.51, 99.66, and 99.88 %, respectively. Remaining SSP or PSSP in the supernatants could be readily removed by the simple modification of the recovery method such as the introduction of the cascade recovery system or the increase of heating time. High R values revealed that most of oligoelectrolytes had participated in the thermally-assisted formation of hydrated gels, indicating that the reuse of the PSSPs is possible without any other energy consuming process, such as membrane distillation or ultrafiltration except for thermal energy. Since it was reported that the remaining amount of draw solute in the supernatant of the precipitated draw solution is constant regardless of an initial concentration of the draw solution [63], R values of SSP and PSSP in the dilute draw solution should not be very different from those obtained using the 20 wt% solutions. The water content of the hydrated gel was analyzed in order to estimate the degree of dehydration of SSP and PSSP above their LCST points. As shown in Table 4.3 and

Figure 4.14, the water content of hydrated gels is about 30 % for both of SSP and PSSPs, indicating that molecular weight does of our sample does not affect the water content. This result could be explained by the presence of hydrophilic sulfonate moieties in SSP and PSSP that can strongly interact with water molecules both in the solution and the hydrated gel, as reported elsewhere [61].

PSSPs having 2 or 3 repeat units such as PSSP2 or PSSP3 might be a better oligomeric system for the draw solute having lager water flux values than PSSP5, PSSP6, and PSSP11 with reasonable reverse salt flux values and high recovery efficiency. However, PSSP2 or PSSP3 could not be easily obtained by the free radical polymerization from SSP because the preparation of polymers with a degree of polymerization of 2 or 3 is known to be possible from telomerization using an efficient chain transfer agent [65]. If the chain transfer agents are included in the polymers with a degree of polymerization of about 2 or 3, then they can be considered as different chemical compounds. The only possible way to prepare structurally similar PSSP2 or PSSP3 is to use the organic synthesis from a proper starting material, while it should be another set of work. Nevertheless, the FO performance results including the easy separation of the PSSPs, clearly indicate that oligomeric PSSPs are efficient draw materials in the FO systems.

To explore the possible use of the PSSP in the desalination application, water permeation flux was measured using 20 wt% solution of PSSP5 as a draw solution and 2000 ppm NaCl solution as a feed solution. The water permeation flux values in AL-FS mode (the feed solution facing the active layer) was of 6.12 LMH which is slightly smaller than that (8.25 LMH) obtained in the deionized water system (Figure 4.15 and 4.16). The smaller water permeation flux value in the NaCl feed solution system could be ascribed to the relatively high osmotic potential of the NaCl feed solution [34,35]. Furthermore the reasonably high water permeation flux was found to be remained using the recycled PSSP5 separated by the same thermal treatment method mentioned above. This recyclability could be ascribed to the stability of the polymer in such mild FO operation and separation conditions; in these temperature and solution conditions, polymers are not much damaged [66,67]. ^{1}H NMR spectra (Figure 4.17) of pristine PSSP5 used at the 1st run and PSSP5 seperated after the 4th run show that their chemical structures are identical. Figure 4.18 and Figure 4.19 further support the recyclability of the polymer in the FO system; osmalality of PSSP5 at 4th run is almost same as that of the prinstine PSSP5, while LCST value slightly increases after the 4th run. The slight increase of LCST might be ascribed to the possible small amount of salt in the polymer not perfectly purified from the thermal separation step. It is well-known that the small amount of salt in the polymer can increase the LCST in the

polymer system.[38] This desalination performance and recycling results clearly shows the possibility to produce enormous quantity of purified water from the brackish water with relatively low energy consumption using the PSSP draw solute system.

Biofouling such as bacteria adhesion has been known as a critical problem in water plants, because the biofilm produced from the attachment of bacteria reduces the overall flow rate and water quality. The bactericidal property of the PSSP series was tested against model negative bacteria (*E. coli*, ATCC 8739) using the shaking flask method,[42] in order to estimate the bactericidal property of the PSSP solution. As shown in Figure 4.20, more than 99.9 % of the calculated bactericidal properties were observed for SSP, PSSP5, PSSP6, and PSSP11, based on the contact of the positively charged tetrabutylphosphonium with the negatively charged bacterial cell [68]. This result provides a clear understanding of a new way to solve the biofouling problem that can occur during the operation of the FO system.

4.4. Conclusion

A series of oligomeric poly(tetrabutylphosphonium styrenesulfonate)s (PSSPs) having the lower critical solution temperature (LCST) behavior were synthesized in order to use them as a draw solute in the forward osmosis (FO) system. Although the water permeation flux values of the oligomeric PSSPs are slightly smaller than those of the monomeric SSP, the reverse solute flux values of the PSSPs were much smaller than those of the SSP, indicating that oligomeric PSSPs are more efficient draw solute system than the monomeric SSP. It is worth noting that more than 99.5% of PSSPs in the solutions can be recovered by only thermal treatment without any further following membrane process or significant decrease in the water permeation flux. About 99.9% of bactericidal properties were observed, due to the presence of the tetrabutylphosphonium cation. Taking our results into consideration, the PSSP is a promising candidate with good FO performances, efficient recovery method, and bactericidal property, which can encourage the design and synthesis of multi-functional draw solute materials.

4.5. References

[1] Cath TY, Childress AE, Elimelech M. J Membr Sci 281 (2006) 70-87.

[2] Hoover LA, Phillip WA, Tiraferri A, Yip NY, Elimelech M. Environ Sci Tech 45 (2011) 9824-9830.

[3] Choi Y-S, Kim K-H, Kim D-G, Kim HJ, Cha S-H, Lee J-C. RSC Adv 40 (2014) 41195-41203.

[4] Kim D-G, Kang H, Choi Y-S, Han S, Lee J-C. Polym Chem 4 (2013) 5065-5073.

[5] Kim D-G, Kang H, Han S, Lee J-C. ACS Appl Mater Interfaces 4 (2012) 5898-5906.

[6] Kim HJ, Baek Y, Choi K, Kim D-G, Kang H, Choi Y-S, Yoon J, Lee J-C. RSC Adv 4 (2014) 32802-32810.

[7] Zhao S, Zou L, Tang CY, Mulcahy D. J Membr Sci 396 (2012) 1-21.

[8] Valladares Linares R, Li Z, Sarp S, Bucs S, Amy G, Vrouwenvelder JS. Water Res 66 (2014) 122-139.

[9] Lutchmiah K, Verliefde AR, Roest K, Rietveld LC, Cornelissen ER. Water Res 58 (2014) 179-197.

[10] Sant'Anna V, Marczak LDF, Tessaro IC. J Food Eng 111 (2012) 483-489.

[11] Wang KY, Teoh MM, Nugroho A, Chung T-S. Chem Eng Sci 66 (2011) 2421-2430.

[12] Yang Q, Wang KY, Chung T-S. Sep Purif Technol 69 (2009) 269-274.

[13] Nagy E. J Membr Sci 460 (2014) 71-81.

[14] Chekli L, Phuntsho S, Shon HK, Vigneswaran S, Kandasamy J, Chanan A. Desalin Water Treat 43 (2012) 167-184.

[15] Li D, Wang H. J Mater Chem A 1 (2013) 14049-14060.

[16] Su J, Chung T-S, Helmer BJ, de Wit JS. J Membr Sci 396 (2012) 92-100.

[17] Wallace M, Cui Z, Hankins NP. Desalination 227 (2008) 34-45.

[18] Achilli A, Cath TY, Childress AE. J Membr Sci 364 (2010) 233-241.

[19] Bowden KS, Achilli A, Childress AE. Bioresource Technol 122 (2012) 20-216.

[20] Zeng Y, Qiu L, Wang K, Yao J, Li D, Simon GP, Wang R, Wang H. RSC Adv 3 (2013) 887-894.

[21] Zhang H, Li J, Cui H, Li F. Chem Eng J 259 (2014) 814-819.

[22] Cai Y, Shen W, Wang R, Krantz WB, Fane AG, Hu X. Chem Commun 49 (2013) 8377-8379.

[23] Ge Q, Su J, Amy GL, Chung T-S. Water Res 46 (2012) 1318-1326.

[24] Ou R, Wang Y, Wang H, Xu T. Desalination 318 (2013) 48-55.

[25] Zhao P, Gao B, Yue Q, Kong J, Shon HK, Liu P, Gao Y. Chem Eng J 273

(2015) 316-324.

[26] Ge Q, Su J, Chung T-S, Amy G. Ind Eng Chem Res 50 (2010) 382-388.

[27] Ling MM, Wang KY, Chung T-S. Ind Eng Chem Res 49 (2010) 5869-5876.

[28] Zhao Q. Chen N, Zhao D, Lu X. ACS Appl Mater Interfaces 5 (2013) 11453-11461.

[29] Cui Y, Ge Q, Liu X-Y, Chung T-S. J Membr Sci 467 (2014) 188-194.

[30] Ge Q, Chung T-S. Chem Commun 49 (2013) 8471-8473.

[31] Guo CX, Zhao D, Zhao Q, Wang P, Lu X. Chem Commun 50 (2014) 7318-7321.

[32] Nakayama D, Mok Y, Noh M, Park J, Kang S, Lee Y. Phys Chem Chem Phys 16 (2014) 5319-5325.

[33] Kim J-j, Chung J-S, Kang H, Yu YA, Choi WJ, Kim HJ, Lee J-C. Macromol Res 22 (2014) 963-970.

[34] Li D, Zhang X, Yao J, Simon GP, Wang H. Chem Commun 47 (2011) 1710-1712.

[35] Altaee A, Zeragoza G, van Tonnigen HR. Desalination 336 (2014) 50-57.

[36] Razmjou A, Liu Q, Simon GP, Wang H. Environ Sci Tech 47 (2013) 13160-13166.

[37] Zaho D, Wang P, Zhao Q, Chen N, Lu X. Desalination 348 (2014) 26-32.

[38] Kohno Y, Deguchi Y, Ohno H. Chem Commun 48 (2012) 11883-11885.

[39] Kohno Y, Ohno H. Aust J Chem 65 (2012) 91-94.

[40] Nishimura N, Ohno H. Polymer 55 (2014) 3289-3297.

[41] Baker JS, Dudley LY. Desalination 118 (1998) 81-89.

[42] Ahn J, Sohn E-H, Bang S, Kang J, Kim T, Hong H, Kim S-E, Kim B-S, Yoon J, Lee J-C. Macromol Res 22 (2014) 337-343.

[43] Choi Y-S, Kang H, Kim D-G, Cha S-H, Lee J-C. ACS Appl Mater Interfaces 6 (2014) 21297-21307.

[44] Lin AH-M, Chang Y-H, Chou W-B, Lu T-J. J Agr Food Chem 59 (2011) 5890-5898.

[45] Omorodion SNE, Hamielec AE, Brash JL. J Liq Chromatogr 4 (1981) 1903-1916.

[46] Rader HJ, Schrepp W. Acta Polymer 49 (1998) 272-293.

[47] Reed JD, Krueger CG, Vestling MM. Phytochemistry 66 (2005) 2248-2263.

[48] Zao S, Zou L. J Membr Sci 379 (2011) 459-467.

[49] Stone ML, Wilson AD, Harrup MK, Stewart FF. Desalination 312 (2013) 130-136.

[50] Lord RCC. Postgrad Med J 75 (1999) 67-73.

[51] Stevens MJ, Kremer K. Phys Rev Lett 71 (1993) 2228-2231.

[52] Yethiraj A. J Phys Chem B 113 (2009) 1539-1551.

[53] Phillip WA, Yong JS, Elimelech M. Environ Sci Technol 44 (2010) 5170-5176.

[54] Ren J, McCutcheon JR. Desalination 343 (2014) 187-193.

[55] Hancock NT, Cath TY. Environ Sci Technol 43 (2009) 6769-6775.

[56] Yen SK, Mehnas Haja NF, Su M, Wang KY, Chung T-S. J Membr Sci 364 (2010) 242-252.

[57] Teraoka I. Polymer solutions: an introduction to physical properties, first ed., John Wiley & Sons, New York, 2002.

[58] Men Y, Li X-H, Antonietti M, Yuan J. Polym Chem 3 (2012) 871-873.

[59] Kohno Y, Ohno H. Phys Chem Chem Phys 14 (2012) 5063-5070.

[60] Lessard DG, Ousalem M, Zhu XX. Can J Chem 79 (2001) 1870-1874.

[61] Men Y, Schlaad H, Voelkel A. Polym Chem 5 (2014) 3719-3724.

[62] Patterson D. Macromolecules 2 (1969) 672-677.

[63] Cai Y, Shen W, Wei J, Chong TH, Wong R, Krantz WB, Fane AG, Hu X. Environ Sci: Water Res Technol 1 (2015) 341-347

[64] Li W, Wu P. Polym Chem 5 (2014) 5578-5590.

[65] Odian G. Principles of Polymerization, fourth ed., John Wiley & Sons, Inc., Hoboken, 2004.

[66] Ge Q, Ling M, Chung T-S. J Membr Sci 442 (2013) 225-237.

[67] Heskins M, Guillet JE. J Macromol Sci Chem 2 (1968) 1441-145.

[68] Akihiko K, Ikeda T, Endo T. J Polym Sci Part A: Polym Chem 31 (1993) 1441-1447.

Table 4.1. Synthesis and properties of tetrabutylphosphonium styrenesulfonate (SSP) and the oligomeric poly(tetrabutylphosphonium styrenesulfonate) (PSSP#)

	Initiator mol%[a]	Molecular weight (Da)[b]	Viscosity (cP)[c]
SSP	-	-	0.996
PSSP5[a]	20	2,100	2.602
PSSP6[a]	5	2,600	2.665
PSSP11[a]	1	4,700	12.615

[a] Mol% of the initiator to the amount of the monomer, tetrabutylphosphonium styrenesulfonate (SSP).
[b] Molecular weights were measured using MALDI-TOF mass spectrometry
[c] Viscosities were measured at 10 wt% concentration.

Table 4.2. Osmotic pressures, water permeation fluxes, and reverse solute fluxes of the SSP and PSSP solutions at various concentrations.

	Osmotic pressure (atm)[a]				Water permeation flux (LMH)[b]		Reverse solute flux (gMH)[b]	
Conc. (wt%)	10	20	30	40	10	20	10	20
SSP	8.79	20.73	32.27	43.11	8.02	16.28	0.29	0.53
PSSP5	8.04	20.85	29.76	42.96	7.58	14.50	0.11	0.14
PSSP6	8.01	19.02	24.69	40.06	7.43	13.66	0.05	0.08
PSSP11	7.16	15.15	22.72	34.44	6.32	13.14	0.01	0.05

[a] Osmotic pressures were obtained using the freezing point depression method.
[b] Water permeation flux and reverse solute flux values were measured using a small-scale custom forward osmosis (FO) system.

Table 4.3. Water content in the hydrated gel separated from the precipitated SSP and PSSP solutions.

	Water content (%)
SSP	30.36
PSSP5	32.78
PSSP6	30.10
PSSP11	32.44

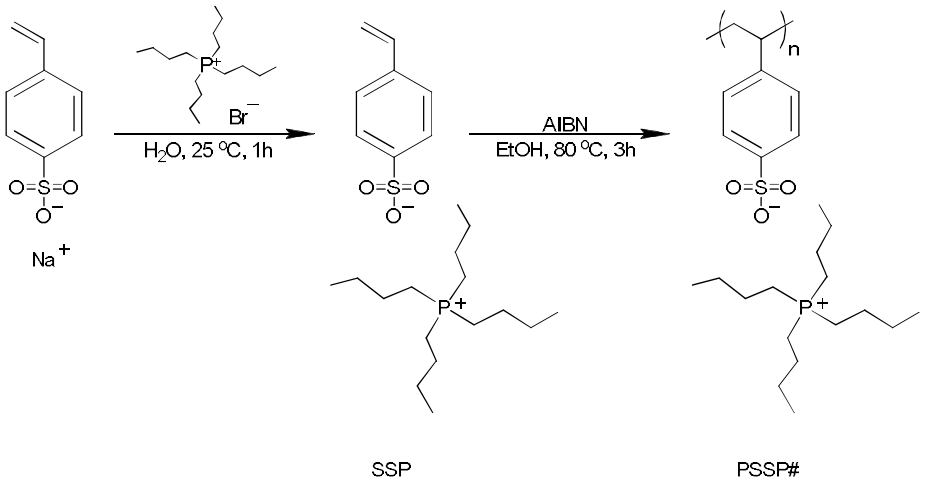

Figure 4.1. Synthesis of tetrabutylphosphonium styrenesulfonate (SSP) and a series of poly(tetrabutylphosphonium styrenesulfonate) (PSSP#, where # is the number of monomer units in the oligomer calculated from the result of MALDI-TOF mass spectrometry).

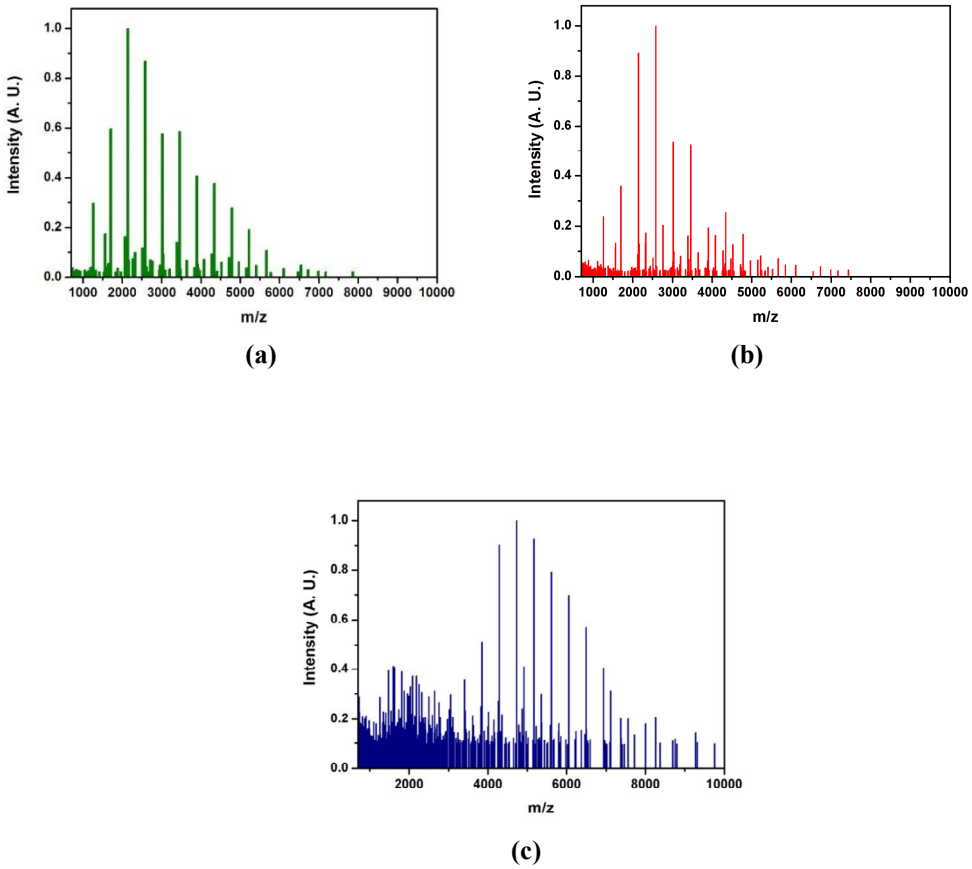

Figure 4.2 MALDI-TOF mass spectra of PSSP series: (A) PSSP5, (B) PSSP6, and (C) PSSP11.

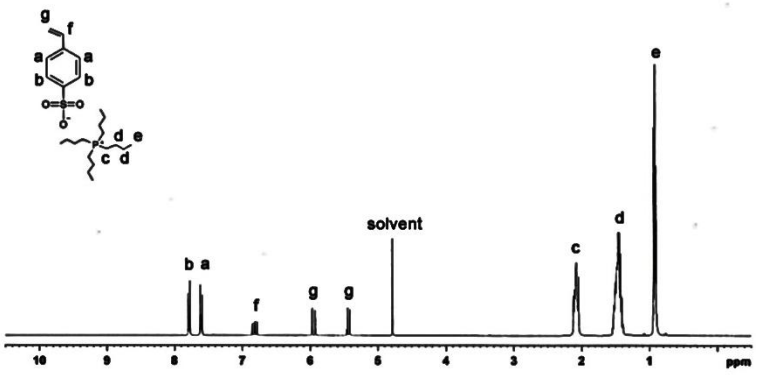

(a)

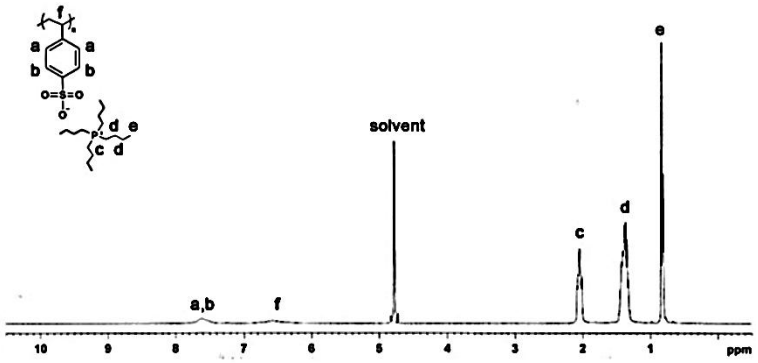

(b)

Figure 4.3 ^{1}H NMR spectra of (a) SSP and (b) PSSP11.

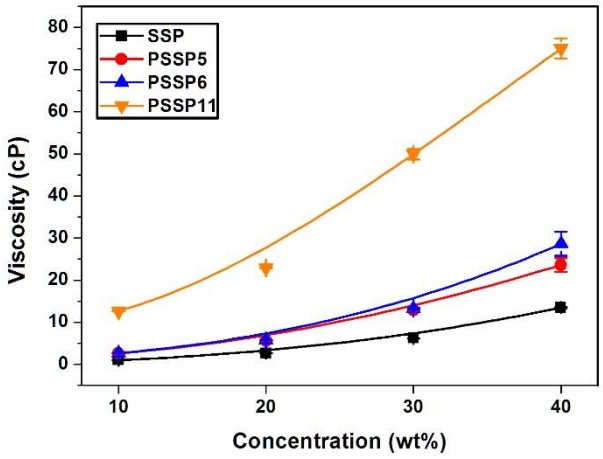

Figure 4.4 Viscosity behavior of SSP, PSSP5, PSSP6, and PSSP11.

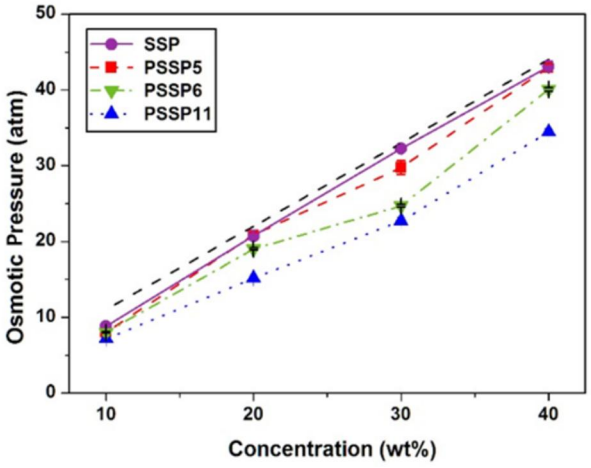

Figure 4.5 Osmotic pressure behavior of SSP, PSSP5, PSSP6, and PSSP11. The predicted osmotic pressures are calculated from the van't Hoff equation, assuming a van't Hoff factor of 2, as represented by the dashed line.

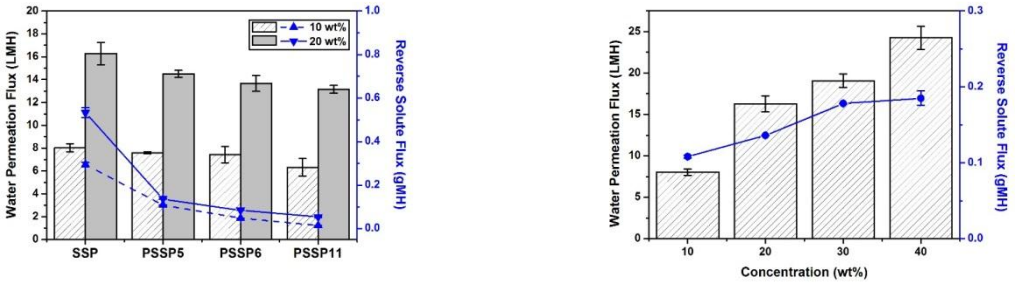

(a) **(b)**

Figure 4.6 (a) Water permeation flux and reverse solute flux of SSP, PSSP5, PSSP6, and PSSP11 at 10 and 20 wt% concentration. (b) Water permeation fluxes and reverse solute fluxes as a function of concentration using the PSSP5 as the draw solute.

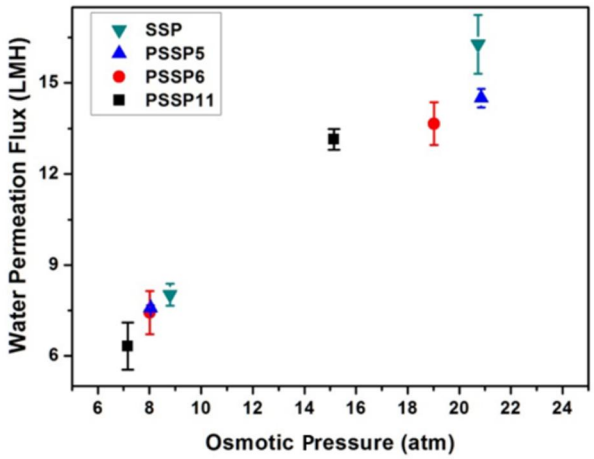

Figure 4.7 Water permeation fluxes of SSP, PSSP5, PSSP6, and PSSP11 of each osmotic pressure value. Water permeation fluxes were measured in the AL-DS mode.

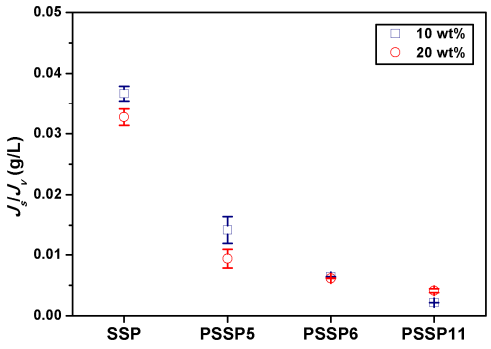

Figure 4.8 J_s/J_v ratio of SSP, PSSP5, PSSP6, and PSSP11.

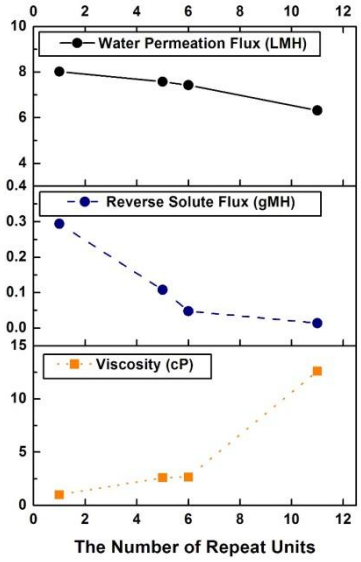

Figure 4.9 Water permeation flux, reverse solute flux, and viscosity of SSP, PSSP5, PSSP6, and PSSP11 as a function of the number of repeat units at 10 wt% concentration.

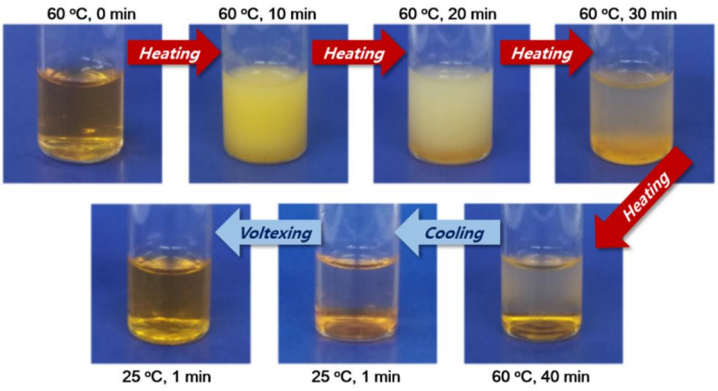

Figure 4.10 Reversible phase transition by heating and cooling the PSSP11 solution in the presence of a small amount of methyl orange dye.

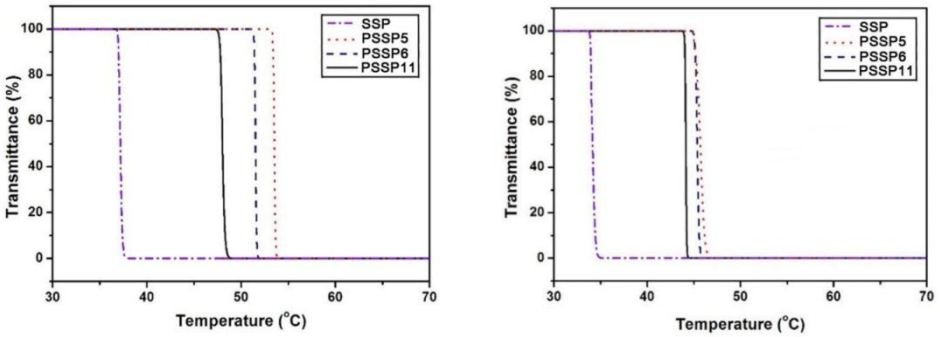

(a) **(b)**

Figure 4.11 Lower critical solution temperature (LCST) results measured (a) at 10 wt% concentration and (b) at 20 wt% concentration.

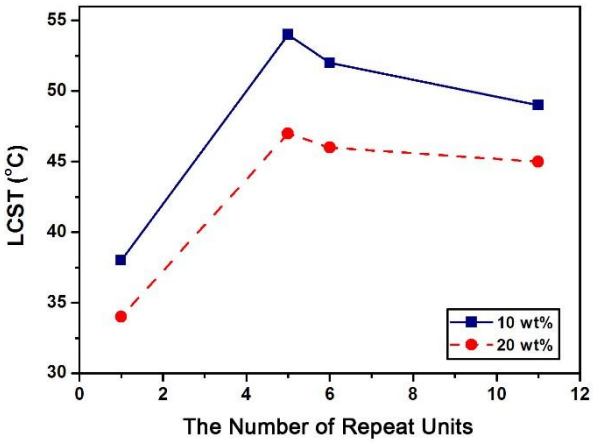

Figure 4.12 The relationship between molecular weight and LCST at each concentration.

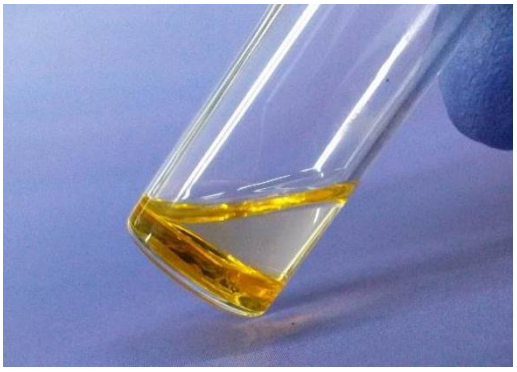

Figure 4.13 Thermo-responsive phase transition of PSSP11 solution in the presence of a small amount of methyl orange dye.

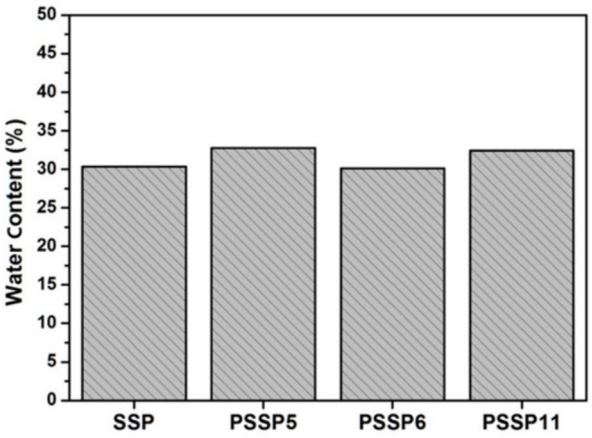

Figure 4.14 Water content in the hydrated gel separated from the precipitated SSP and PSSP solutions.

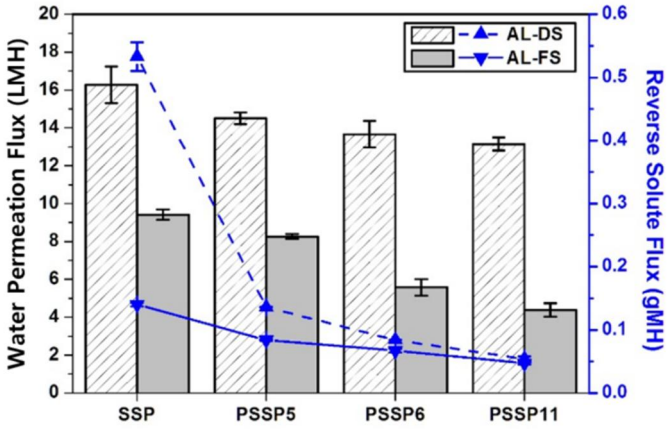

Figure 4.15 Water permeation flux and reverse solute flux of SSP and the PSSP# series at different membrane orientation.

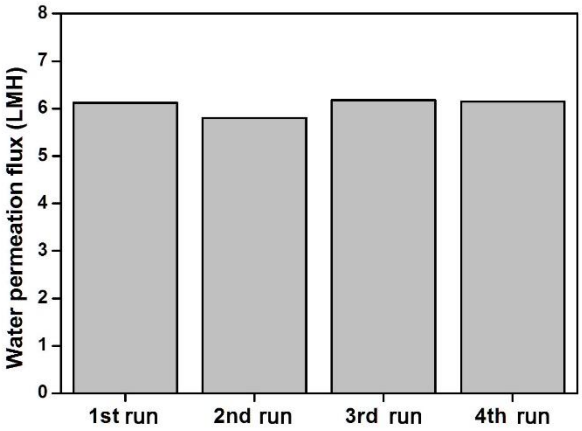

Figure 4.16 Water permeation fluxes results using 20 wt% solution of PSSP5 as a draw solution and 2000 ppm NaCl solution as a feed solution. From the 2nd to the 4th run, the recovered PSSP5 from the previous run was used.

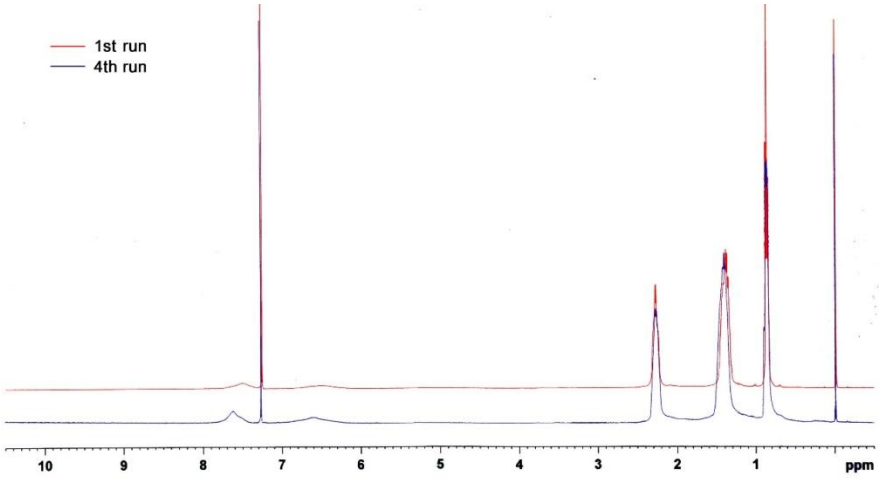

Figure 4.17 ^{1}H NMR spectra of pricitine PSSP5 used at the 1st run and PSSP5 seperated after the 4th run.

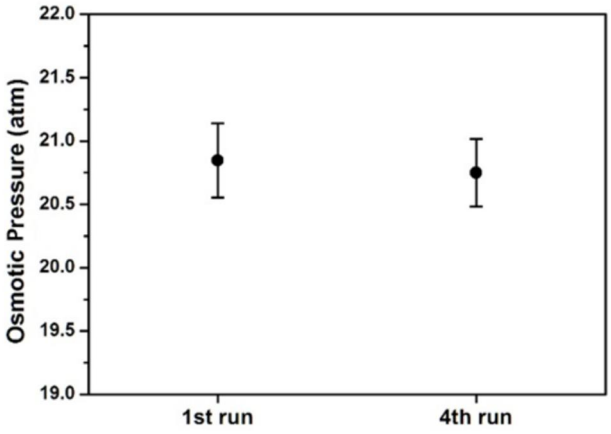

Figure 4.18 osmotic pressures using 20 wt% solution of PSSP5 as a draw solution and 2000 ppm NaCl solution as a feed solution. From the 2nd to the 4th run, the recovered PSSP5 from the previous run was used.

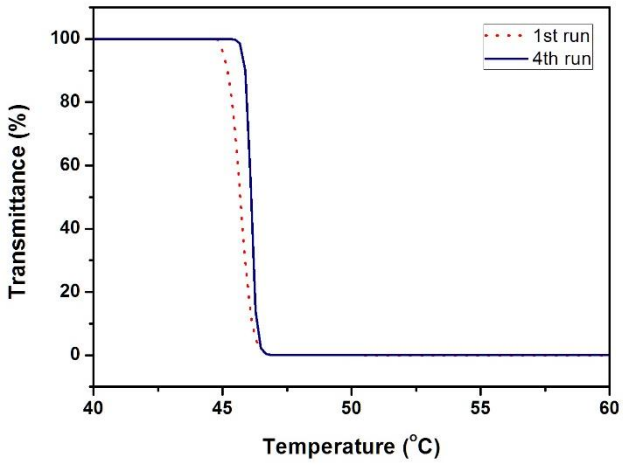

Figure 4.19 LCST using 20 wt% solution of PSSP5 as a draw solution and 2000 ppm NaCl solution as a feed solution. From the 2nd to the 4th run, the recovered PSSP5 from the previous run was used.

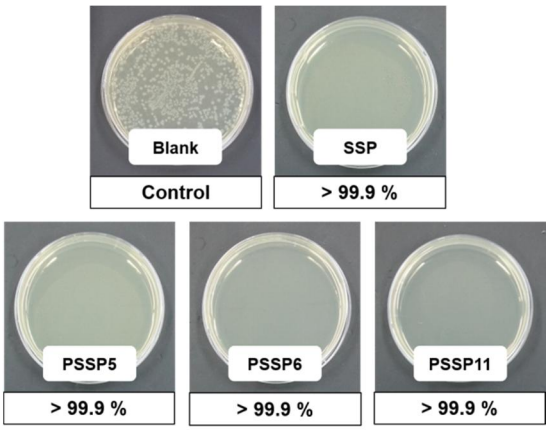

(a)

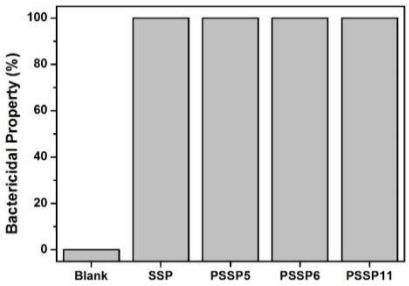

(b)

Figure 4.20 Results of antibacterial test of the blank sample and the PSSP series: (a) Photographic results and (b) bactericidal rates.

초 록

본 연구에서는 수처리 공정에 사용될 수 있는 여러 고분자 재료에 대한 합성 및 분석에 대하여 기술하였다. 첫째로, 홍합으로부터 기인된 친수성의 도파민과 폴리술폰을 기반으로 한 한외여과용 수처리막을 그래프팅-쓰루 중합 및 비용매 유도 상분리법으로 구성된 단일공정으로 제조하였다. 이후 항균성 저분자 펩타이드인 니신에 분리막을 침지하여 도파민의 카테콜 작용기와 니신간 공유결합을 형성하여, 최종적으로 항균성과 방오성능을 동시에 지니는 수처리막을 구성하였다. 형성된 수처리막들은 도파민 작용기로 인한 높은 친수성과 이로 인한 방오 성능을 나타내었으며, 니신 작용기로 인하여 그람 양성균에 대한 높은 항균성을 나타내었다.

둘째, 지지체 및 폴리아미드 박막분리층으로 구성된 박막복합체 (thin film composite) 을 형성하였다. 지지체의 경우 폴리술폰과 다이메틸아미노에틸 메타크릴레이트 (DMAEMA)간 그래프팅-쓰루 중합 및 단일공정상의 비용매 유도 상분리법을 통해 형성하였으며, 형성한 다공성 지지체는 폴리술폰 지지체와 유사한 구조를 가지면서도 높은 친수성을 나타내는 것을 확인하였다. 이후 1,3,5-트리메조일 클로라이드

및 *m*-페닐렌디아민간의 계면중합을 통해 지지체 위에 폴리아미드 박막분리층을 형성하였으며, 최종적으로 형성한 박막분리층을 1,3-프로판술폰 용액에 침지시켜 DMAEMA 의 아민 작용기를 양쪽성 술포베타인 작용기로 전환시켜 양쪽성 이온을 포함하는 박막복합체를 형성하였다. 형성한 박막 복합체는 지지체의 친수성으로 인하여 정삼투 공정에서 비슷한 수준의 역방향 염투과도상에서 크게 증가된 수투과도를 나타내었으며, 친수성 및 양쪽성 지지체로 인하여 본 연구에서 형성된 박막복합체는 비교군인 폴리술폰 지지체로 구성된 박막복합체에 비해 높은 방오성능을 나타내었다.

마지막으로, 올리고머 계열의 분자량을 지니는 폴리테트라부틸포스포늄-스티렌술포네이트(PSSP)를 합성하여 이를 정삼투 공정용 유도 용질로 사용하고자 하였다. 합성한 올리고머는 구조내에 이온쌍을 지니고 있어 수용액 상에서 높은 삼투압을 보이면서도, 그 자체의 경계적 친수성으로 인하여 가열 시 하이드로겔을 형성하며 침전하는 현상을 보였다. 이러한 PSSP의 온도감응성은 정삼투 공정에서의 유도 용질 재사용 공정의 용이성을 부여하게되며, 하이드로겔 형성으로 인하여 유도 용질 재사용 공정 시 단순히 상층액을 분리해내는 저에너지 공정의 사용을 가능하게 하므로 정삼투 공정의 에너지 소모량을 비약적으로 감소시킬

수 있었다.

주요어: 수처리, 수처리 분리막, 유도 용질, 정삼투, 한외여과, 방오성, 항균성

학번: 2010-23327 성명 : 김진주